J. Fluid Mech. (1981), *vol.* 113, *pp.* 187–220
Printed in Great Britain

A vortex sheet modelling of boundary-layer noise

By J. E. FFOWCS WILLIAMS AND M. PURSHOUSE
Cambridge University Engineering Department, Trumpington Street, Cambridge CB2 1PZ

(Received 20 July 1979 and in revised form 3 November 1980)

In this paper we describe a simple way of modelling boundary-layer effects in analytical flow noise studies. We develop an exact analogy between the real flow and one in which there is a step velocity profile. This profile is intended to model a boundary layer in an idealized way and we recognize it in our Green's function for the problem. We insist that the Green's function is bounded, a step that makes it non-causal and similar to those used in recent jet-noise analogies. We derive an expression for the induced pressure which consists of surface and volume terms, just as in Lighthill's theory, but, because both contain elements to be evaluated in future time, we argue that the turbulence must be able to respond to linear surface stimulus and avoid the otherwise inevitable violation of causality. This novel feature distinguishes our analysis from applications of Lighthill's theory to boundary-layer-induced noise. The response of the turbulence may be large when the surface is driven at low boundary-layer Strouhal number. But it is negligible at high Strouhal number, and in that limit the surface terms are found to depend only on the instantaneous boundary geometry and its rate of change. This leads to a simple expression for 'boundary-layer fluid loading', in which the finite boundary-layer scale emerges explicitly. To illustrate the physical consequences of this result, we use it to estimate the impedance of a baffled piston vibrating beneath a boundary layer. Potential theory predicts that flow should destabilize the piston motion while experiments usually indicate the reverse. We find that the boundary layer is responsible for the discrepancy and that experimentally observed behaviour is predicted quite reasonably by our model.

1. Introduction

Mean flow effects rarely feature in analytical studies of turbulent-boundary-layer noise. The mean flow is often assumed to be irrelevant if it is at low Mach number, and the noise is estimated by modelling the boundary layer as a region of turbulence adjacent to a supporting surface embedded in an otherwise stationary acoustic medium (Lighthill 1952; Powell 1960; Ffowcs Williams 1965, 1966, 1972).

By ignoring the mean flow, models such as these overlook some important effects. For instance, the impedance of acoustic liners such as those used to silence noisy flow ducts is known to be influenced by the adjacent mean flow, and that can make it difficult to estimate from measurements taken in static tests a liner's likely effectiveness in an application (Meyer, Mechel & Kurtze 1958; Mechel 1960). If the flow induces the instability of the surface that supports it, it introduces a type of surface motion altogether more violent than any found in models that neglect it. Benjamin (1964) has shown how flow can destabilize a homogeneous, elastic surface, and Ffowcs Williams & Lovely (1975) have since described how potential flow destabilizes a

spring-mounted piston set in a rigid, plane baffle. In that case the motion is divergent if the flow-induced suction on the proud piston exceeds the restoring force offered by the spring. Flow-induced instabilities such as these could well be extremely noisy, but analytical difficulties have so far defeated attempts to find out whether they are (Lovely 1974).

Some important acoustical consequences of introducing a mean flow can of course be brought out explicitly by applying the appropriate form of Lighthill's (1952) acoustic analogy, when, instead of developing the theory of a medium at rest, the medium is given uniform motion and the flow represented as a uniform potential flow with slip over the surface that supports it. This was the view that Ffowcs Williams & Lovely took. Boundary-layer effects are ignored, but that is not obviously serious because the modelling is correct over most of the flow and fails only within a thin layer adjacent to the surface.

In fact a suitable modelling of that layer is more important than it appears, largely because conditions there have such a major influence on the pressures on the adjacent surface, pressures that play an important part in determining how that surface will respond when it is excited. Ffowcs Williams & Lovely illustrated the basic weakness of potential theory when they showed that, according to the theory's linearized form, the flow-induced force on a sharp-edged, baffled piston displaced from the baffle plane is infinite. Analysis with no linearizing assumptions reveals that the force is actually finite, but that its magnitude can be changed markedly by making trivial alterations to the piston edge geometry. This type of behaviour, where the pressures reached at the piston corners are limited only by how sharp the corners are, is a characteristic of a potential modelling that would surely not be expected in a real flow, where the piston is submerged beneath a relatively stagnant boundary layer. Indeed, there are serious doubts that even the sign of the flow-induced force is correctly predicted by the potential modelling. The dynamics of Ffowcs Williams & Lovely's spring-mounted piston are analogous to those of a baffled Helmholtz resonator of the type used in the construction of flow duct acoustic liners, and there are now a number of reported instances in which, far from reducing the natural frequency of such a resonator, as would be expected from potential-theory results, the flow actually increases it (see, for example, Meyer *et al.* 1958; Mechel 1960; Panton & Miller 1975; Anderson 1977). There is evidently a pressing need for a more representative theory. The boundary layer plays a vital role, but it is one that cannot be discerned from a straightforward application of Lighthill's theory.

In this paper we explore these distinctive boundary-layer features through an analysis which models the boundary layer explicitly, albeit in an idealized way. We develop an exact analogy between the real flow and one in which the mean velocity is zero at and up to a finite distance from the supporting boundary. Beyond that, the mean velocity is taken to be constant and equal to the free-stream velocity of the real flow. Consequently, our model recognizes that there is a buffer zone between the supporting surface and the main flow, a buffer that effectively cushions the flow from small-amplitude movements of the boundary.

The analysis has much in common with recent jet noise analogies in which the generation of turbulence-induced sound is modelled in terms of sources positioned next to a vortex sheet (Ffowcs Williams 1974; Mani 1976; Dowling, Ffowcs Williams & Goldstein 1978). Our step profile is without doubt the simplest conceivable model of a

boundary layer, but it may be thought to be a somewhat naïve one. More intuitively plausible schemes based on smoother mean shear profiles could certainly be devised, but they are less obviously to be preferred to the somewhat cruder model that we are proposing than might at first be supposed. For the instantaneous velocity field in a turbulent boundary layer is far from being a small perturbation of the mean, particularly in the boundary layer's near-surface equilibrium layer, where the fluctuating components of velocity amount to some 20–30% of the local mean values (see Townsend 1976, pp. 260 and 291). The velocity profile with which the surface interacts at any instant is unlikely ever to resemble the mean. Indeed, it is the relatively large velocity fluctuations within a boundary layer that make possible the 'local' Kelvin–Helmholtz instabilities that induce the bursts and sweeps that maintain the turbulent field, instabilities that are lost in a modelling based on a gradual mean shear profile if the chosen profile is stable to small disturbances (and the mean profiles encountered in practice usually are (Landahl 1967)). Instabilities could be introduced by the deliberate choice of an unstable mean profile, of course, but the profile selection would inevitably be a somewhat arbitrary procedure. In the absence of compelling reasons to the contrary, the best choice of profile under these circumstances may well be the one that admits the boundary layer's existence in the simplest possible way.

Aside from its relative simplicity, the vortex sheet model has a further attraction, because aeroacoustic theories that identify sound sources with inhomogeneous departures from a mean profile also suffer from fundamental, and so far unresolved, difficulties of principle. These schemes follow in essentials the analysis first developed by Lilley (1974) by arranging the equations of motion in a way that collects linear terms on the left-hand side and nonlinear fluctuating terms on the right-hand side. The right-hand-side terms are identified as sources of sound, but it is difficult to specify rigorously the field that those sources induce, because non-trivial solutions exist that satisfy the left-hand side though they do not rely on non-zero right-hand-side terms for their existence. Consequently, to obtain practical results of the type reported by Morfey & Tester (1976), which showed encouraging agreement with experiment, certain elements of the solution have to be discarded, a procedure that is difficult to justify. By contrast, vortex sheet analogies are based, like Lighthill's theory, on simple wave equations for which uniqueness theorems provide the essential justification for identifying terms that appear on the right-hand side as sources of sound (Dowling *et al.* 1978).

Only time will tell whether one particular model profile, supported by rigorous analytical procedures, can be shown to be superior in all respects to the alternatives. But for the present, the success achieved by vortex sheet analogies in estimating jet noise certainly makes the idea of exploring how far similar ideas might be exploited in a boundary-layer application a very attractive one. That is essentially what this paper is about. Although in fact we develop our analogy for the case of an incompressible fluid, we keep a firm eye on aeroacoustic applications. Some of the analogy's most important distinctive features turn out to be connected with the incompressible part of the flow and are thus most easily studied in this simplified theory. This is not to underrate in any way the importance of fluid compressibility-related effects, but they are wholly additional to those we report here.

There is an unstable 'vortex sheet' in our model, so that we face a choice between the causal, unbounded, or the non-causal, bounded Green's function in the analysis.

In fact we require the bounded Green's function that does not conform to strict causality, and in consequence our integral expression for the induced pressure contains elements that are to be evaluated over all time, past and future. The integrals in the jet noise analogies are of course of the same type, and they invite the simple interpretation, apparently obviously wrong, that a source can be 'heard' before it has fired. Jet flow sources, though, are defined to be in turbulence formed at the unstable interface between stationary and moving fluids, and the motion of individual turbulent eddies not only generates sound; it also triggers off further instability which results in yet more turbulence later on. It is this noisy evolution of turbulence that appears as a precursor to the actual turbulent sources, and it is found in all acoustic analogies which include the influence of an unstable mean flow. This rather unusual source structure does not seriously hamper interpretation of the theory in applications to free jets, and apparently significant new dimensional laws which characterize the sound sources and their radiation directivity can be deduced quite simply (Mani 1976; Dowling *et al.* 1978).

In our boundary-layer application, where surface terms play a key role, the causality question is far more important. Its mere existence is at first sight surprising because it is unusual in incompressible flow studies of this type for there to be any time dependence at all. In incompressible flow the acoustic analogy formally reduces to Poisson's equation, solutions to which are normally determined by the instantaneous flow and boundary conditions. The main structure in our results comes from the important dynamical features that are introduced by the instabilities of the turbulence-generating shear flow. Surface and volume terms cannot now be handled separately as they usually are in applications of Lighthill's theory, where the turbulent field is taken, e.g. in Curle (1955), to be fixed irrespective of any boundary movement in the vicinity. To assume this in our non-causal analogy is to imply that the field at any instant can be influenced by an arbitrary boundary movement later on. That would be nonsense. Causality of the complete problem requires that the sum of the surface and turbulence source terms that have to be evaluated in future time must be absolutely fixed. The turbulence must therefore be determined to some extent by surface motion. This prediction, that turbulence must respond to linear surface forcing, is a hint that boundary-layer turbulence may well respond to applied stimuli in a way essentially similar to that in which jets are now known to do (Moore 1977).

We give particular emphasis in this paper to situations in which the boundary movements are imposed externally, and try to estimate the pressure induced on the surface. In doing so we examine the turbulence response that the boundary movements induce and consider under what circumstances that response is important, and when it is negligible. We find that only when there are grounds for supposing that the boundary movements do not perturb the turbulence is it possible to give a simple description of fluid-loading effects.

The turbulence is likely to respond vigorously when the flow-supporting boundary oscillates at frequencies low in comparison with the boundary layer's characteristic frequency, particularly when the flow is stimulated by surface wave elements that share the phase speed of its instabilities. But the turbulence is effectively decoupled from the surface at high Strouhal number, and in this limit the various terms in the integral expression for the pressure can be given a familiar interpretation. The volume terms are taken to represent the turbulence field, as usual, and they still contain

elements in future time, but the surface terms now depend only on the geometry of the surface and its time derivatives at the observation time. We interpret these surface terms as boundary-layer fluid loading. They have a distinctive structure.

As a definite illustration of the field to be expected when boundary-layer effects are admitted, we apply this result to Ffowcs Williams & Lovely's (1975) problem of the estimation of the impedance of a baffled piston under a boundary layer. The results confirm their prediction that in the large-piston limit the flow-induced piston force is a suction limited by the finite boundary-layer scale. But the most interesting results concern pistons of somewhat smaller diameter. For these pistons which, incidentally, cover almost the entire range of sizes which might be used to model the cavity resonators used in acoustic liners, the mean flow-induced force has a sign opposite to that found by Ffowcs Williams & Lovely. The flow induces a compressive force on a piston standing proud of its baffle, a restoring force which tends to drive the piston back to a position flush with the baffle. This force is equivalent to a stiffness, and would induce an increase in the resonance frequency of a spring-mounted piston. This result is actually consistent with the observed behaviour of acoustic liners under flow and, furthermore, the resonance frequency shifts that are found in practice are in reasonable agreement with what we would anticipate from our model.

2. The flow

We consider a situation in which a turbulent boundary layer is formed at the interface between a steady flow and an almost planar supporting surface as shown in figure 1. The surface is in a state of small-amplitude vibration, driven either by the flow or by externally applied stresses, and we wish to estimate the induced pressure in the flow.

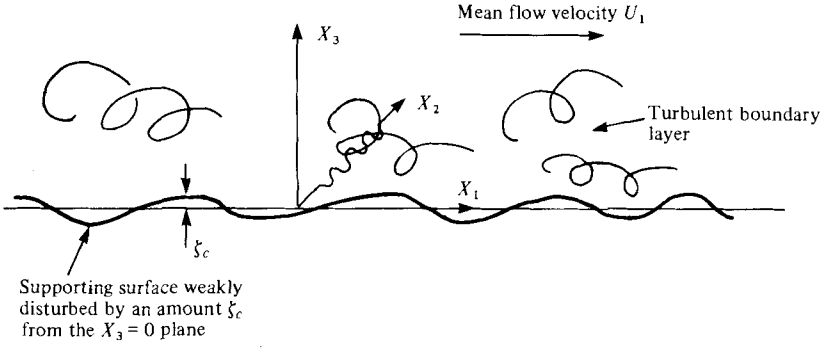

FIGURE 1. A slightly non-planar flexible surface supports a uniform mean flow and is separated from it by a turbulent boundary layer.

3. Lighthill's theory

In incompressible flow the pressure satisfies a Poisson equation

$$\nabla_y^2 p = -\frac{\partial^2(\rho u_i u_j)}{\partial y_i \partial y_j},$$

where ρ is the density and u_i the velocity. This equation can be 'solved' by using the corresponding Green's function G which satisfies

$$\nabla_{\mathbf{y}}^2 G = \delta(\mathbf{x}-\mathbf{y}).$$

G is defined to be sufficiently well behaved at infinity for repeated integration by parts, so that the pressure within the fluid-filled volume V can be expressed in terms of the Reynolds-stress distribution within the volume and the boundary conditions at the supporting surface, C:

$$p(\mathbf{x},t) = -\int_V \rho u_i u_j \frac{\partial^2 G}{\partial y_i \partial y_j}\, dV - \int_C \left(p\frac{\partial G}{\partial n} - \rho G \frac{\partial u_n}{\partial t}\right) dS. \tag{3.1}$$

The suffix n denotes the direction of the outward-facing normal and viscous terms are assumed negligible.

The compressible form of this equation is the starting point for many analytical studies of boundary-layer noise (Powell 1960; Ffowcs Williams 1965, 1966, 1972; Crighton 1968). The volume terms are assumed to provide a description of a turbulent field that is taken to be fixed irrespective of conditions at the supporting boundary. Boundary effects are to be inferred from the surface terms. But the volume terms contain also an implicit description of mean flow effects in an extensive linear distribution of sources and the scheme of analysis cannot distinguish between those effects and genuine turbulence. A different approach is needed to separate the two.

An obvious way of minimizing the importance of the steady flow-related volume terms is to develop the analysis in terms of the difference $u_i' = u_i - U_1\delta_{i1}$ between the actual velocity field u_i and the steady velocity $U_1\delta_{i1}$ remote from the surface, a procedure that leads to the expression

$$p(\mathbf{x},t) = -\int_V \rho u_i' u_j' \frac{\partial^2 G}{\partial y_i \partial y_j}\, dV - \int_C \left(p\frac{\partial G}{\partial n} - \rho G \frac{Du_n'}{Dt}\right) dS. \tag{3.2}$$

D/Dt signifies the convective time derivative defined by

$$\frac{D}{Dt} = \frac{\partial}{\partial t} + U_1 \frac{\partial}{\partial y_1}.$$

Because the Reynolds stress is now based on the difference between the actual velocity and that of the steady flow remote from the boundary, extensive volume terms linear in the fluctuating velocity field are impossible, and the regions of significant Reynolds stress are more obviously associated with those of the boundary-layer turbulence. Mean flow effects have a separate identity because they are now described by surface terms, and indeed equation (3.2) is the only formulation in which those effects can be brought out explicitly. Boundary-layer effects, though, remain implicit; now they are inextricably linked with the volume terms that describe the turbulence, in the form of linear elements that have to be evaluated in the region near to the supporting surface.

4. The boundary-layer modelling

The object of the modelling described in the pages which follow is to draw together both these formulations of the incompressible version of Lighthill's theory so that the best features of each are built into a single framework in which the existence of an

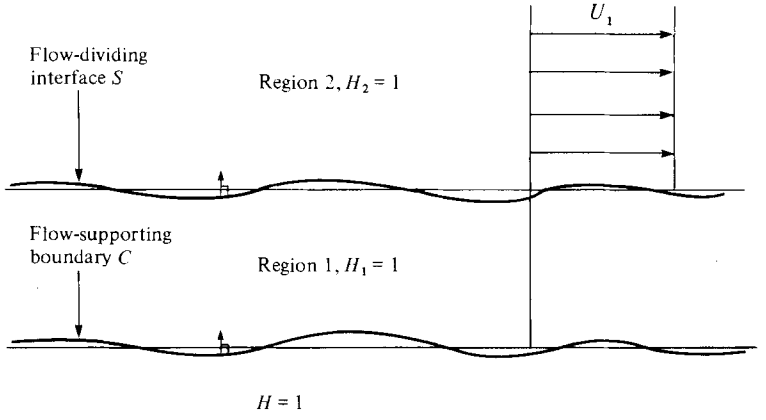

FIGURE 2. The flow division used in the boundary-layer modelling. $H_2 = 1$ in region 2 and the analysis is based on the difference u_i between the actual velocity u_i and that of the flow remote from the boundary, $U_1\delta_{i1}$. $H_1 = 1$ in region 1 where the analysis is based on the actual velocity field, i_i. In the rest of space $H = 1$.

idealized boundary layer is made quite explicit. We divide the flow into two regions, 1 and 2, as shown in figure 2, and then obtain expressions for the pressure in each region using the form of Lighthill's theory which is most appropriate to that region.

In the near-surface region 1, we develop the analysis in terms of the actual velocity field u_i. In region 2, which comprises the flow more remote from the surface where the velocity ultimately reaches the steady value $U_1\delta_{i1}$, we work in terms of the velocity difference $u_i' = u_i - U_1\delta_{i1}$. Each region is identified with a corresponding Heaviside function defined to be unity within the region and zero outside it. H_1 defines region 1 and H_2 region 2, so that the volume for which $H_1 + H_2 = H = 1$ defines the whole space occupied by the fluid. These Heaviside functions are chosen to be constant on any one fluid particle, so that particles do not cross from one region of the fluid to the other. S marks the boundary between the two fluid regions and C that between the fluid and the rest of space.

The pressure within each region is given in terms of the Reynolds stress within the fluid and the pressure and normal particle velocity at the region's boundaries by Goldstein (1977, p. 166), so that, in our problem, the pressure in region 1 is given by

$$H_1 p(\mathbf{x}, t) = \int_\infty \left[-H_1 \rho u_i u_j \frac{\partial^2 G_1}{\partial y_i \partial y_j} + \rho u_i \frac{\partial H_1}{\partial y_i}\frac{\partial G_1}{\partial \tau} - p\frac{\partial G_1}{\partial y_i}\frac{\partial H_1}{\partial y_i}\right] d^3\mathbf{y}\, d\tau \qquad (4.1)$$

and in region 2 by

$$H_2 p(\mathbf{x}, t) = \int_\infty \left[-H_2 \rho u_i' u_j' \frac{\partial^2 G_2}{\partial y_i \partial y_j} + \rho u_i' \frac{\partial H_2}{\partial y_i}\frac{DG_2}{D\tau} - p\frac{\partial G_2}{\partial y_i}\frac{\partial H_2}{\partial y_i}\right] d^3\mathbf{y}\, d\tau, \qquad (4.2)$$

where G_1 and G_2 are the two elements of the Green's function, G,

$$G = H_1 G_1 + H_2 G_2,$$

and they satisfy Poisson equations in their respective regions:

$$H_1 \nabla_{\mathbf{y}}^2 G_1 = H_1 \delta(\mathbf{x} - \mathbf{y})\delta(t - \tau); \quad H_2 \nabla_{\mathbf{y}}^2 G_2 = H_2 \delta(\mathbf{x} - \mathbf{y})\delta(t - \tau).$$

The pressure at any point in the flow, $Hp(\mathbf{x}, t)$, is equal to the sum of (4.1) and (4.2),

and we can write the result in a slightly simplified form because of our stipulation that H_1 and H_2 are associated with individual fluid particles:

$$\frac{\partial H_1}{\partial \tau} + u_i \frac{\partial H_1}{\partial y_i} = \frac{DH_2}{D\tau} + u_i' \frac{\partial H_2}{\partial y_i} = 0,$$

$$Hp(\mathbf{x}, t) = \int_\infty \left[-H_1 \rho u_i u_j \frac{\partial^2 G_1}{\partial y_i \partial y_j} - H_2 \rho u_i' u_j' \frac{\partial^2 G_2}{\partial y_i \partial y_j} + p \left(\frac{\partial G_1}{\partial y_i} - \frac{\partial G_2}{\partial y_i} \right) \frac{\partial H_2}{\partial y_i} \right.$$
$$\left. - \rho \left(\frac{DH_2}{D\tau} \frac{DG_2}{D\tau} - \frac{\partial H_2}{\partial \tau} \frac{\partial G_1}{\partial \tau} \right) + p \frac{\partial G_1}{\partial y_i} \frac{\partial \bar{H}}{\partial y_i} - \rho u_i \frac{\partial \bar{H}}{\partial y_i} \frac{\partial G_1}{\partial \tau} \right] d^3\mathbf{y}\, d\tau. \quad (4.3)$$

Here $\bar{H}$ is a further Heaviside function, defined to be unity in the space not occupied by the fluid, and as before we have neglected viscous terms.

The linear surface terms on S depend on the field induced by both the turbulence and the surface vibration, so that their estimation is likely to be both difficult, and extremely sensitive to errors. We therefore eliminate them by imposing constraints on the Green's function and require that

$$\int_\infty p \left(\frac{\partial G_1}{\partial y_i} - \frac{\partial G_2}{\partial y_i} \right) \frac{\partial H_2}{\partial y_i} d^3\mathbf{y}\, d\tau = 0 \quad (4.4)$$

and

$$\int_\infty \left(\frac{DH_2}{D\tau} \frac{DG_2}{D\tau} - \frac{\partial H_2}{\partial \tau} \frac{\partial G_1}{\partial \tau} \right) d^3\mathbf{y}\, d\tau = 0. \quad (4.5)$$

Equation (4.4) is satisfied by the continuity of normal gradient

$$\frac{\partial G_1}{\partial y_i} \frac{\partial H_2}{\partial y_i} = \frac{\partial G_2}{\partial y_i} \frac{\partial H_2}{\partial y_i},$$

while (4.5), which with a sufficiently good Green's function we can integrate by parts into the form

$$\int_\infty H_2 \left(\frac{D^2 G_2}{D\tau^2} - \frac{\partial^2 G_1}{\partial \tau^2} \right) d^3\mathbf{y}\, \partial\tau = 0,$$

imposes a jump in the Green's function such that

$$\frac{\partial^2 G_1}{\partial \tau^2} = \frac{D^2 G_2}{D\tau^2}$$

in region 2.

These constraints help specify the Green's function and allow equation (4.3) to be written in a simplified form. The pressure is expressed as the sum of volume terms to be evaluated over the whole flow and surface terms on the physical supporting boundary:

$$Hp(\mathbf{x}, t) = \int_\infty \left[T + \left(p \frac{\partial G_1}{\partial y_i} - \rho u_i \frac{\partial G_1}{\partial \tau} \right) \frac{\partial \bar{H}}{\partial y_i} \right] d^3\mathbf{y}\, d\tau, \quad (4.6)$$

where

$$T = -H_1 \rho u_i u_j \frac{\partial^2 G_1}{\partial y_i \partial y_j} - H_2 \rho u_i' u_j' \frac{\partial^2 G_2}{\partial y_i \partial y_j}.$$

The volume terms in this equation are free of linear elements both in the turbulence-free flow beyond the boundary layer and in the region near to the supporting surface, so that this equation suffers from neither of the drawbacks in the two formulations of

Lighthill's theory, and yet the volume terms continue to provide a description of the turbulent velocity fluctuations. Thus the existence of a rudimentary boundary layer is now recognized explicitly in the Green's function, though that is still not completely specified. Further constraints can be imposed at the bounding surface of the flow.

Though the terms in equation (4.6) have a familiar form, they must in fact be interpreted very carefully because the constraints we have applied to the Green's function have already given it considerable structure. We now consider those constraints more closely and examine their consequences when the formal and exact analogy of equation (4.6) is used to calculate the pressure field in incompressible boundary-layer flow.

5. The Green's function – its similarity to the vortex sheet Green's function

The two elements of the Green's function, G, satisfy Poisson equations,

$$H_1 \nabla_{\mathbf{y}}^2 G_1 = H_1 \delta(\mathbf{x}-\mathbf{y})\,\delta(t-\tau); \quad H_2 \nabla_{\mathbf{y}}^2 G_2 = H_2 \delta(\mathbf{x}-\mathbf{y})\,\delta(t-\tau),$$

to which solutions must be chosen so that across S the derivatives normal to S are continuous,

$$[1] \qquad \frac{\partial G_1}{\partial n_S} = \frac{\partial G_2}{\partial n_S}$$

and such that

$$[2] \qquad \frac{\partial^2 G_1}{\partial \tau^2} = \frac{D^2 G_2}{D\tau^2}$$

throughout region 2. We may constrain either G_1, or $\partial G_1/\partial n_C$ at the supporting boundary, C, as a third condition [3], while the fourth [4] condition implied in the analysis requires that $G(\mathbf{y},\tau|\mathbf{x},t) \to 0$ as $|\mathbf{y},\tau| \to \infty$.

Our immediate interest concerns the jump conditions [1] and [2] to be satisfied across S. The second of them may not appear to be a surface condition, but its parentage, revealed by equation (4.5), shows that it is. Here we shall ensure that condition [2] is satisfied specifically at S, and will merely assert that it holds throughout region 2, a step that is permissible because G_2 is undefined in that region and so can be assigned any value there. Our jump conditions do, in fact, have essentially the same structure as those used by Dowling *et al.* (1978) in their jet noise modelling (see their equation (3.1)).

There are obvious difficulties connected with the conditions at the flow-dividing interface because the exact position of that interface is impossible to specify. The distance between the interface and the flow-supporting boundary must be related in some way to the physical boundary-layer scale, though the amount by which the mean flow is displaced from the surface will usually be much exaggerated by taking the interface height as the boundary-layer thickness. We shall argue later that the buffer depth may reasonably be identified with the boundary layer's much smaller displacement thickness.

For the present we need to specify the interface geometry only in general terms, and in a way that renders the analysis tractable. Accordingly we shall assume that the interface is only weakly disturbed from a mean plane that is defined to be at a fixed distance d from the undisturbed flow-supporting boundary plane $y_3 = 0$. We can then

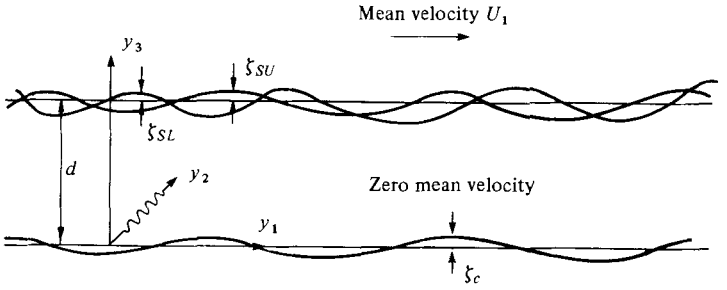

FIGURE 3. In this hypothetical situation, a flow with unperturbed mean velocity U occupies $y_3 > d+\zeta_{SU}$; quiescent fluid occupies $\zeta_c < y_3 < d+\zeta_{SL}$.

linearize the boundary conditions to be applied on S and apply them instead at the mean plane.

Now, to see that the jump conditions [1] and [2] have the same structure as the jump conditions across a vortex sheet, consider figure 3, which shows a hypothetical situation in which a potential flow is, like our boundary-layer modelling, divided into two regions. In one, at distances $y_3 > d+\zeta_{SU}$ the unperturbed flow velocity is $U_1\delta_{i1}$, while in the other, $\zeta_c < y_3 < d+\zeta_{SL}$, the mean velocity is zero. A discontinuous sheet separates the two flow regions and the sheet's upper and lower surfaces are displaced in the y_3-direction by small amounts ζ_{SU} and ζ_{SL} respectively. Like a real flow, this one is supported on a boundary which is assumed to be only weakly disturbed by an amount ζ_c from its mean position in the $y_3 = 0$ plane.

The potential field within each region of this hypothetical flow is related to the boundary displacements in the usual way. If the flow-dividing interface is to represent a vortex sheet then, firstly, the displacements at its upper and lower surfaces must be the same,

$$\zeta_{SU} = \zeta_{SL} \tag{5.1}$$

and, secondly, there must be no pressure discontinuity across it.

We can compare these constraints with those to be applied to our Green's function if we write the latter in terms of a function ψ defined by

$$G_{1,2} = \int^{y_3} \psi_{1,2}\, dy_3.$$

The jump conditions that we insist must be satisfied across S in our formal analogy may be written in terms of ψ as

$$\psi_1 = \psi_2 \tag{5.2}$$

and

$$\frac{\partial^2}{\partial\tau^2}\int^{y_3}\psi_1 dy_3 = \frac{D^2}{D\tau^2}\int^{y_3}\psi_2 dy_3. \tag{5.3}$$

If ψ is interpreted as the fluid particle displacement in the y_3-direction then (5.3) is actually the pressure-continuity condition and the jump conditions we impose on G at the interface S are the jump conditions across a vortex sheet.

The Green's function may also feature the mechanical properties of the physical flow-supporting surface, C, if G and $\partial G/\partial n_c$ are appropriately constrained there, as in

effect they would have to be in applications to the study of sound generation by flow over passive compliant surfaces (see Ffowcs Williams 1965). In the case when the surface motion is specified, the essential structure of G is that of a vortex sheet boundary layer formed on a rigid boundary.

There is an obvious limit to the utility of this physical picture, though, because the fourth condition on G demands its boundedness, and that could not be satisfied in a physical realization of a vortex sheet flow. A vortex sheet is unstable to disturbances at all finite wavenumbers, so that a source positioned next to it would induce a response which grows without limit, a result which applies also to the vortex sheet flows formed on flexible surfaces (see Benjamin 1964). The causal Green's functions for those flows are therefore unsuitable for our analysis.

Jones (1973), Morgan (1975) and later Dowling *et al.* (1978) have all observed that boundedness can be ensured in exact analogies which feature unstable 'vortex sheets' only by relaxing the causality condition, because only then is it possible to ensure that G is zero at both large positive and large negative values of its arguments. The use of this Green's function means that some of the source elements on the right-hand side of equation (4.6) are to be evaluated in future time, a feature that is the hallmark of unstable flow analogies, and one which we think has significant implications for the interpretation of that equation.

6. Turbulence and the vibration of a supporting boundary may interact strongly

Because the sources on the right-hand side of equation (4.6)

$$Hp(\mathbf{x},t) = \int_{\infty} \left[T + \left(p \frac{\partial G_1}{\partial y_i} - \rho u_i \frac{\partial G_1}{\partial \tau} \right) \frac{\partial \bar{H}}{\partial y_i} \right] d^3\mathbf{y}\, d\tau \qquad (4.6\ bis)$$

contain elements to be evaluated in future time, that equation cannot be handled in the same way as the corresponding expression in Lighthill's theory. The possibility of a nonsensical result is made obvious when the surface vibrations are driven externally, the Green's function constrained such that

$$\frac{\partial G_1}{\partial y_i} \frac{\partial \bar{H}}{\partial y_i} = 0$$

and equation (4.6) written in the form

$$Hp(\mathbf{x},t) = \int_{\infty} \left[T - \rho u_i \frac{\partial G_1}{\partial \tau} \frac{\partial \bar{H}}{\partial y_i} \right] d^3y\, d\tau. \qquad (6.1)$$

The surface terms now depend only on the velocity distribution of the bounding surface, but equation (6.1) requires that that distribution must be specified at all times, including times later than the observation time t. This seems absurd, because boundary movements are subject to independent control, and it is inconceivable that the induced pressure within the flow could really depend on how those movements are configured at some future time.

The flaw in the argument is that causality restrictions do not apply to the individual source terms; they apply only to their sum. So, if one of the source terms is subject to independent control, as the surface terms in equation (6.1) clearly are, then there will

be no breach of causality provided that the remaining terms respond to the control in such a way as to preserve the causality of the sum. That response can come only from the volume terms that we have taken to describe the turbulent field, so it is evident that in our analogy, unlike in Lighthill's, it cannot be assumed that the 'turbulent' volume terms remain uninfluenced by movement of the boundary.

To see this, contrast the turbulence development in the following two situations. In the first, the boundary follows some prescribed non-zero vibration in the whole time interval from $-\infty$ to $+\infty$. In the second, the boundary vibrations are exactly the same up to some time t' later than the observation time t. Thereafter the boundary is deliberately held rigid during the subsequent time interval from t' to ∞. The pressure fields in both situations must be identical at time t, so that the source terms that describe the turbulence development from t' to $+\infty$ in the first case,

$$\int_{\infty}\int_{t'}^{\infty}[T]\,d^3\mathbf{y}\,d\tau,$$

when the boundary vibration is maintained for all time, must differ from those that occur when the boundary is deliberately held rigid during that time interval,

$$\int_{\infty}\int_{t'}^{\infty}[T_R]\,d^3\mathbf{y}\,d\tau,$$

say, by an amount equal to the surface source terms that occur in the vibrating surface case:

$$\int_{\infty}\int_{t'}^{\infty}\rho u_i\frac{\partial G_1}{\partial\tau}\frac{\partial\bar{H}}{\partial y_i}\,d^3\mathbf{y}\,d\tau=\int_{\infty}\int_{t'}^{\infty}[T-T_R]\,d^3\mathbf{y}\,d\tau.$$

These surface terms might integrate to zero in some circumstances but they will not do so in general. There must therefore be a turbulence response to boundary movement, a response that is of first order in the boundary movement. This is in marked contrast to conventional aeroacoustic theory, where turbulence is regarded as a fixed source of excitation and where it is assumed that the scattering effect of a boundary positioned adjacent to it can be deduced from the surface terms alone. Our analogy suggests that surface effects might actually be linked inextricably with changes of comparable importance in the turbulent field itself, so that applications of the theory to boundary-layer noise problems may well call for very careful interpretation.

It would be surprising though if turbulence response were always important, and in a first study such as this it is natural to try to identify the types of boundary movement that induce the extremes of large and small response. We turn attention to these aspects in the next section, where we consider the development of a turbulent boundary layer formed on a surface whose movements we can control completely.

7. The pressure field within a boundary layer formed on a deliberately forced, compliant surface

When the boundary movements are specified independently of the flow, the appropriate Green's function is that for an instability-free vortex sheet boundary layer formed on a rigid, plane boundary, so that our next step is to calculate that Green's function.

7.1. *The Green's function for an instability-free vortex sheet boundary layer formed on a rigid, plane boundary*

The Green's function satisfies

$$\nabla_{\mathbf{y}}^2 G_1 = \delta(\mathbf{x}-\mathbf{y})\,\delta(t-\tau) \quad \text{in} \quad 0 < y_3 < d, \tag{7.1}$$

$$\nabla_{\mathbf{y}}^2 G_2 = \delta(\mathbf{x}-\mathbf{y})\,\delta(t-\tau) \quad \text{in} \quad y_3 > d, \tag{7.2}$$

is subject to the constraints

$$\left.\begin{aligned} &[1] \quad \frac{\partial G_1}{\partial y_3} = \frac{\partial G_2}{\partial y_3} \\ &[2] \quad \frac{\partial^2 G_1}{\partial \tau^2} = \frac{D^2 G_2}{D\tau^2} \end{aligned}\right\} \quad \text{at} \quad y_3 = d,$$

$$[3] \quad \frac{\partial G_1}{\partial y_3} = 0 \quad \text{at} \quad y_3 = 0,$$

and we must choose the solution such that

[4] both G_1 and G_2 are bounded.

We take Fourier transforms in (y_1, y_2, τ) and so write equations (7.1) and (7.2) in the form

$$\left(-|\mathbf{k}|^2 + \frac{\partial^2}{\partial y_3^2}\right)\tilde{G}_{1,2}(\mathbf{k}, \omega, y_3|\mathbf{x}, t) = \delta(x_3 - y_3)\, e^{i\mathbf{k}.\mathbf{x}+i\omega t}. \tag{7.3), (7.4}$$

At this stage we are mainly interested in the pressure induced near the surface, so we will focus attention on cases in which the observation point $\mathbf{x}$ lies in the near-surface region 1 (though of course the analysis could be developed in just the same way for an observer positioned in the other region). Solutions $\tilde{G}_1$ and $\tilde{G}_2$ which satisfy (7.3) and (7.4) may then be written

$$\tilde{G}_1(\mathbf{k}, \omega, y_3|\mathbf{x}, t) = Ae^{|\mathbf{k}|y_3} + Be^{-|\mathbf{k}|y_3} - \frac{\exp[i\mathbf{k}.\mathbf{x} + i\omega t - |\mathbf{k}|\,|x_3 - y_3|]}{2|\mathbf{k}|},$$

$$\tilde{G}_2(\mathbf{k}, \omega, y_3|\mathbf{x}, t) = Ce^{|\mathbf{k}|y_3} + De^{-|\mathbf{k}|y_3},$$

where A, B, C and D are independent of y_3 and are to be determined from the boundary conditions. By applying conditions [1], [2] and [3], and by taking inverse transforms in $(\mathbf{k}, \omega)$, G_1 and G_2 can be written as

$$\begin{aligned} G_1(\mathbf{y}, \tau|\mathbf{x}, t) = {} & -\frac{\delta(t-\tau)}{4\pi}\left[\frac{1}{|\mathbf{x}-\mathbf{y}|} + \frac{1}{|\mathbf{x}^*-\mathbf{y}|}\right] \\ & -\frac{1}{(2\pi)^3}\int_{\infty} \frac{(2u_1\omega k_1 + U_1^2 k_1^2)\exp i\mathbf{k}.(\mathbf{x}-\mathbf{y}) + i\omega(t-\tau) - 2|\mathbf{k}|d]}{4|\mathbf{k}|\,[\omega^2 + \tfrac{1}{2}(1-e^{-2|\mathbf{k}|d})\,(2U_1\omega k_1 \times U_1^2 k_1^2)]} \\ & \times (e^{-|\mathbf{k}|(x_3-y_3)} + e^{|\mathbf{k}|(x_3+y_3)} + e^{-|\mathbf{k}|(y_3-x_3)} + e^{-|\mathbf{k}|(x_3+y_3)} d^2\mathbf{k}\, d\omega, \end{aligned} \tag{7.5}$$

$$\begin{aligned} G_2(\mathbf{y}, \tau|\mathbf{x}, t) = {} & -\frac{\delta(t-\tau)}{4\pi}\left[\frac{1}{|\mathbf{x}-\mathbf{y}|} + \frac{1}{|\mathbf{x}^*-\mathbf{y}|}\right] \\ & +\frac{1}{(2\pi)^3}\int_{\infty} \frac{(2U_1\omega k_1 + U_1^2 k_1^2)\,(1-e^{-2|\mathbf{k}|d})\,e^{i\mathbf{k}.(\mathbf{x}-\mathbf{y})+i\omega(t-\tau)}}{4|\mathbf{k}|\,[\omega^2 + \tfrac{1}{2}(1-e^{-2|\mathbf{k}|d})\,(2U_1\omega k_1 + U_1^2 k_1^2)]} \\ & \times (e^{-|\mathbf{k}|(y_3-x_3)} + e^{-|\mathbf{k}|(x_3+y_3)} d^2\mathbf{k}\, d\omega; \end{aligned} \tag{7.6}$$

$\mathbf{x}^*$ denotes the image of $\mathbf{x}$ in the plane $x_3 = 0$. So far the evaluation of G is straightforward, but now care is needed in the ω-integration because that must be performed in such a way that $G(\mathbf{y}, \tau|\mathbf{x}, t) \to 0$ as $|\mathbf{y}, \tau| \to \infty$.

The relevant integral with respect to ω may be written

$$\mathscr{I} = \int_{-\infty}^{+\infty} \frac{e^{i\omega(t-\tau)}\,d\omega}{[\omega^2 + \frac{1}{2}(1-e^{-2|\mathbf{k}|d})(2U_1\omega k_1 + U_1^2 k_1^2)]},$$

and we evaluate it by contour integration, noting that the poles are located at the roots of

$$\omega^2 + \tfrac{1}{2}(1-e^{-2|\mathbf{k}|d})(2u_1\omega k_1 + u_1^2 k_1^2) = 0.$$

For all real, finite k_1, there is a simple pole in each of the upper and lower halves of the complex ω-plane, as shown in figure 4 (*a*).

Because our analysis demands that G be bounded, in the integration with respect to ω we must choose the integration contours sketched out in figure 4 (*b*). The required contours run along the real ω axis and are closed in the upper or lower half planes according as τ is less than or greater than t, so that each contour encloses one pole and there are no indentations. For comparison, contours that would yield the causal Green's function are shown in figure 4 (*c*), where, in order to ensure that G remains zero for $\tau > t$, the contour closed in the lower half plane must be indented so as to exclude the pole located within that half plane. By the same indentation that pole is located in the upper half plane contour and is responsible for the unbounded growth of G as $\tau \to -\infty$. It is this behaviour that prevents our using the causal Green's function in our analogy.

Using the integration contours indicated in figure 4 (*b*), the integration with respect to ω in equation (7.5) may be performed, with the result

$$\begin{aligned} G_1(\mathbf{y}, \tau|\mathbf{x}, t) = {} & -\frac{\delta(t-\tau)}{4\pi}\left[\frac{1}{|\mathbf{x}-\mathbf{y}|} + \frac{1}{|\mathbf{x}^*-\mathbf{y}|}\right] \\ & - \frac{U_1}{(2\pi)^2}\int_{\infty} \frac{|k_1|}{4|\mathbf{k}|} \exp\left[-U_1\beta(ik_1(t-\tau) + \alpha|k_1|\,|t-\tau|) + i\mathbf{k}.(\mathbf{x}-\mathbf{y}) - 2|\mathbf{k}|d\right] \\ & \times \left(\frac{e^{-2|\mathbf{k}|d}}{(1-e^{-4|\mathbf{k}|d})^{\frac{1}{2}}} + i\,\mathrm{sgn}\,(k_1)\,\mathrm{sgn}\,(t-\tau)\right) \\ & \times (e^{-|\mathbf{k}|(x_3-y_3)} + e^{|\mathbf{k}|(x_3-y_3)} + e^{-|\mathbf{k}|(x_3+y_3)} + e^{-|\mathbf{k}|(x_3+y_3)})d^2\mathbf{k}, \end{aligned} \tag{7.7}$$

where $\alpha = (\coth(|\mathbf{k}|d))^{\frac{1}{2}}$ and $\beta = \frac{1}{2}(1-e^{-2|\mathbf{k}|d})$. The integration with respect to ω in equation (7.6) yields an expression for G_2 which has a similar structure

$$\begin{aligned} G_2(\mathbf{y}, \tau|\mathbf{x}, t) = {} & -\frac{\delta(t-\tau)}{4\pi}\left[\frac{1}{|\mathbf{x}-\mathbf{y}|} + \frac{1}{|\mathbf{x}^*-\mathbf{y}|}\right] \\ & + \frac{U_1}{(2\pi)^2}\int_{\infty} \frac{|k_1|}{4|\mathbf{k}|}(1-e^{-2|\mathbf{k}|d}) \exp\left[-U_1\beta(ik_1(t-\tau) + \alpha|k_1|\,|t-\tau|) + i\mathbf{k}.(\mathbf{x}-\mathbf{y})\right] \\ & \times \left(\frac{e^{-2|\mathbf{k}|d}}{(1-e^{-4|\mathbf{k}|d})^{\frac{1}{2}}} + i\,\mathrm{sgn}\,(k_1)\,\mathrm{sgn}\,(t-\tau)\right)(e^{-|\mathbf{k}|(y_3-x_3)} + e^{-|\mathbf{k}|(x_3+y_3)})d^2\mathbf{k}. \end{aligned}$$

Both elements G_1 and G_2 of G contain a term

$$-\frac{\delta(t-\tau)}{4\pi}\left[\frac{1}{|\mathbf{x}-\mathbf{y}|} + \frac{1}{|\mathbf{x}^*-\mathbf{y}|}\right],$$

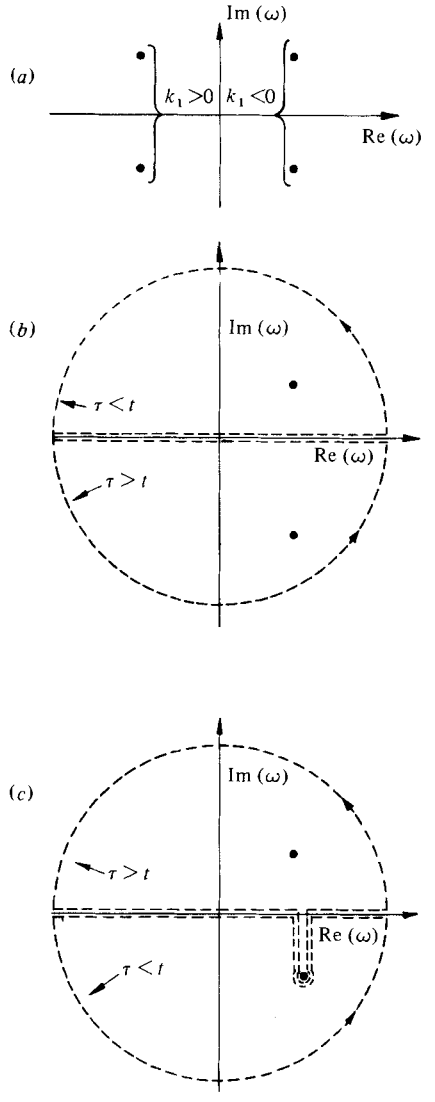

FIGURE 4. The contour integration of equation (7.3). (*a*) Roots of the denominator in the complex ω-plane. (*b*) Our choice of integration contours. Poles for $k_1 < 0$ are shown. (*c*) Integration contours which would yield the causal Green's function. Poles for $k_1 < 0$ are shown.

which is the Green's function for a half space. But they also include a more complicated mean-flow-related term that has non-causal time dependence. In this term the integrand rises and falls with $|t-\tau|$ according to

$$e^{-U_1\alpha\beta|k_1|\,|t-\tau|}$$

and it is this part of G that ensures that convolution integrals such as (4.6) contain elements that have to be evaluated in future time.

7.2. *The turbulence response induced by boundary motion*

We are likely to be able to estimate the pressure induced by forced boundary motion only if it is described by surface terms. Volume terms describe the turbulent field and, if the boundary motion perturbs that field significantly, there is no guarantee that an accurate estimate of boundary effects can be deduced from the surface terms alone. Source elements that characterize the turbulence response could be important.

We know that surface terms to be evaluated in future time must be in some way related to turbulence response, because we are free to configure the surface movement after the observation time in any way we like, without influencing the pressure at the observation time, turbulence-response source terms providing the necessary cancelling field required to prevent what would otherwise be a violation of causality. For this reason it seems unlikely that an identification of boundary effects with surface terms will always be possible.

On the other hand, it would be surprising if there were a significant turbulence response to boundary motion under all circumstances. The boundary layer has a definite characteristic time scale δ/U_1, where δ is a boundary-layer length scale, and U_1 the free-stream velocity, and, if the boundary oscillations are fast on that scale, a significant turbulence response seems unlikely, one oscillation of the boundary being complete long before the boundary layer has time to respond to it. Consequently, were the boundary movements sufficiently rapid, we might expect to find that the surface terms would be of a type that did not suggest a significant turbulence response, and that it might indeed even be possible to write down a simple expression for the surface terms valid in cases where the turbulence was not perturbed. The error involved in approximating the surface terms in this way in any particular case might therefore provide a plausible means of identifying whether turbulence response is important in that case.

This idea finds explicit support in our model, because although the pressure must in general be expressed as

$$Hp(\mathbf{x},t) = \int_{\infty} \{[T]+f(\zeta(\mathbf{y},\tau))\}d^3\mathbf{y}\,d\tau, \tag{7.8}$$

a form which demands a specification of the boundary geometry at all times, this expression simplifies greatly when the boundary is driven at high frequency. In that limit, the pressure may be written as

$$Hp(\mathbf{x},t) = \int_{\infty} [T]\,d^3\mathbf{y}\,d\tau + g(\zeta(\mathbf{y},t)), \tag{7.9}$$

where the boundary geometry has to be specified only at the observation time t. Surface terms that depend on the boundary geometry at other times can be neglected because they are negligible in comparison with those retained.

At the other extreme, when the boundary is held rigid, though not necessarily flat, for all time, the induced pressure

$$Hp(\mathbf{x},t) = \int_{\infty} [T]\,d^3\mathbf{y}\,d\tau$$

is independent of the detailed boundary geometry, because in that limit the surface terms we neglected in equation (7.9) cancel completely the surface terms that were

retained in that equation. Boundary layers formed on surfaces vibrating at finite frequency must in general be dealt with by using the full expression (7.8), and it seems likely that the surface-driven case will be tractable only if that exact expression can reasonably be approximated by equation (7.9) above. In that expression we have discarded the surface terms that depend in the main on the surface geometry at times other than the observation time because they are negligible in comparison with the terms retained; by discarding them we lose the requirement for a turbulence response, because equation (7.9) gives us no grounds for presuming that there is a turbulence response to boundary movement. Therefore, a plausible procedure for estimating the likely significance of turbulence response is to determine the error introduced by writing the surface terms in the simplified form indicated in equation (7.9).

We now consider the Green's function in more detail so that we can identify the characteristics of the boundary motion needed to ensure that the induced pressure is expressible in a form such as (7.9). We focus attention on the pressure induced on the boundary, $x_3 = 0$; this useful simplification does not restrict the validity of the conclusions reached.

The surface terms in equation (6.1),

$$p_s(\mathbf{x}, t) = -\int_\infty \rho u_i \frac{\partial \bar{H}}{\partial y_i} \frac{\partial G_1}{\partial \tau} d^3\mathbf{y}\, d\tau$$

may be written in the linearized approximation as

$$p_s(\mathbf{x}, t) = \int_\infty \rho \frac{\partial \zeta}{\partial \tau} \frac{\partial G_1}{\partial \tau} d^2\mathbf{y}\, d\tau = -\rho \int_\infty \zeta(\mathbf{y}, \tau) \frac{\partial^2 G_1}{\partial \tau^2} d^2\mathbf{y}\, d\tau. \tag{7.10}$$

The elements of G_1 that contain delta functions are of particular interest because those terms can be integrated with respect to τ directly to yield the terms dependent on boundary geometry at time t. We therefore write out $\partial^2 G_1/\partial \tau^2$ in a form that will make those terms quite explicit,

$$\begin{aligned}
\frac{\partial^2 G_1}{\partial \tau^2}(\mathbf{y}, \tau | \mathbf{x}, t) = & -\frac{\partial^2}{\partial \tau^2}\left[\frac{\delta(t-\tau)}{2\pi|\mathbf{x}-\mathbf{y}|}\right] \\
& -\frac{\partial^2}{\partial y_1 \partial \tau}\left[\frac{U_1}{2\pi^2}\delta(t-\tau)\int_\infty \frac{e^{i\mathbf{k}.(\mathbf{x}-\mathbf{y})-2|\mathbf{k}|d}}{|\mathbf{k}|} d^2\mathbf{k}\right. \\
& -\frac{U_1^2}{8\pi^2}\int_\infty \frac{|k_1|}{|\mathbf{k}|}\frac{(1+2e^{-2|\mathbf{k}|d})(1-e^{-2|\mathbf{k}|d})}{(1-e^{-4|\mathbf{k}|d})^{\frac{1}{2}}} \\
& \left.\times \exp\left[-U_1\beta(ik_1(t-\tau)+\alpha|k_1|\,|t-\tau|)+i\mathbf{k}.(\mathbf{x}-\mathbf{y})\right]\times e^{-2|\mathbf{k}|d} d^2\mathbf{k}\right] \\
& -\frac{\partial^2}{\partial y_1^2}\left[-\frac{U_1^2}{4\pi^2}\delta(t-\tau)\int_\infty \frac{(1-2e^{-2|\mathbf{k}|d})}{|\mathbf{k}|} e^{-2|\mathbf{k}|d+i\mathbf{k}.(\mathbf{x}-\mathbf{y})} d^2\mathbf{k}\right. \\
& +\frac{U_1^3}{16\pi^2}\int_\infty \frac{|k_1|}{|\mathbf{k}|}(1-2e^{-2|\mathbf{k}|d})(1-e^{-2|\mathbf{k}|d}) \\
& \times (i\,\mathrm{sgn}\,(k_1)\,\mathrm{sgn}\,(t-\tau)+\alpha)\exp\left[-U_1\beta(ik_1(t-\tau)+\alpha|k_1|\,|t-\tau|)+i\mathbf{k}.(\mathbf{x}-\mathbf{y})\right] \\
& \left.\times e^{-2|\mathbf{k}|d} d^2\mathbf{k}\right].
\end{aligned} \tag{7.11}$$

These elements that contain delta functions, which we may write

$$\frac{\partial^2 G_{1\delta}}{\partial\tau^2}(\mathbf{y},\tau|\mathbf{x},t) = -\frac{\partial^2}{\partial\tau^2}\left[\frac{\delta(t-\tau)}{2\pi|\mathbf{x}-\mathbf{y}|}\right] - \frac{\partial^2}{\partial y_1\partial\tau}\left[\frac{U_1\delta(t-\tau)}{2\pi^2}\int_\infty \frac{e^{i\mathbf{k}.(\mathbf{x}-\mathbf{y})-2|\mathbf{k}|d}}{|\mathbf{k}|}\,d^2\mathbf{k}\right] - \frac{\partial^2}{\partial y_1^2}\left[-\frac{U_1^2\delta(t-\tau)}{4\pi^2}\int_\infty \frac{(1-2e^{-2|\mathbf{k}|d})}{|\mathbf{k}|}e^{-2|\mathbf{k}|d+i\mathbf{k}.(x-y)}\,d^2\mathbf{k}\right] \quad (7.12)$$

make a contribution to the pressure

$$ps_\delta(\mathbf{x},t) = -\rho\int_{\infty,\,y_3=0}\zeta(\mathbf{y},\tau)\frac{\partial^2 G_{1\delta}}{\partial\tau^2}\,d^2\mathbf{y}\,d\tau,$$

and this may be shown, by substitution for $\partial^2 G_{1\delta}/\partial\tau^2$ from equation (7.12) and by integration by parts with respect to (y_1,τ) as appropriate, to be equivalent to

$$p_{s\delta}(\mathbf{x},t) = \frac{\rho}{2\pi}\int_\infty \frac{\partial^2\zeta}{\partial t^2}(\mathbf{y},t)\frac{\partial^2 y}{|\mathbf{x}-\mathbf{y}|} + \frac{\rho}{2\pi}\int_\infty 2U_1\frac{\partial^2\zeta}{\partial y_1\partial\tau}(\mathbf{y},t)\frac{d^2\mathbf{y}}{4d^2+|\mathbf{x}-\mathbf{y}|^2} - \frac{\rho U_1^2}{2\pi}\int_\infty \frac{\partial^2\zeta}{\partial y_1^2}(\mathbf{y},t)\left[\frac{1}{(4d^2+|\mathbf{x}-\mathbf{y}|^2)^{\frac{1}{2}}} - \frac{1}{(16d^2+|\mathbf{x}-\mathbf{y}|^2)^{\frac{1}{2}}}\right]d^2\mathbf{y}. \quad (7.13)$$

These are the surface terms that we expect to apply in cases in which the boundary vibration does not perturb the turbulent field. They have a boundary-layer structure characterized by the length scale d, a structure which vanishes when d is formally set equal to zero, when equation (7.13) reduces to the corresponding expression that occurs in Lighthill's theory,

$$p_{s\delta}(\mathbf{x},t) = \frac{\rho}{2\pi}\int_\infty \left(\frac{\partial}{\partial t}+U_1\frac{\partial}{\partial y_1}\right)^2\zeta(\mathbf{y},t)\frac{d^2\mathbf{y}}{|\mathbf{x}-\mathbf{y}|}.$$

so that there is a direct analytical connection between the terms in (7.13) and those found in the Lighthill theory.

The other elements of $\partial^2 G_1/\partial\tau^2$ depicted in equation (7.11) determine the importance of surface sources to be evaluated primarily at times other than the observation time, and we must now determine under what circumstances those terms are important. We have already arranged the elements of $\partial^2 G_1/\partial\tau^2$ in a way that will enable us to do this. Although that arrangement is not the only one possible, the analysis does actually lead to a natural pairing of the form shown, in which each delta function element is linked with an element that has a more diffuse time dependence. The main justification for 'pairing off' the delta function contributions in the form shown is that these delta function elements lead to surface terms that have a structure very similar to those found in Lighthill's theory, in that they are proportional to $\partial^2\zeta/\partial t^2$, $\partial^2\zeta/\partial y_1\partial\tau$ and $\partial^2\zeta/\partial y_1^2$. We want to compare the magnitude of each of these terms with the source terms that depend on the same surface derivatives, but that are to be evaluated at times other than the observation time. We already know the relative magnitudes of the two types of terms taken as a whole in the limits of low- and high-frequency boundary vibration, so that it makes sense to pair off the individual elements in such a way that those elements have the same asymptotic structure as the surface terms as a whole. Thus there should be no net contribution from any of the pairs when the boundary vibrates at vanishingly small frequency. Conversely, the diffuse time

dependence surface terms must vanish at high enough frequency, ensuring the pre-eminence of the Lighthill type of surface terms in that limit. It was these requirements that led to the pairing of the elements of $\partial^2 G_1/\partial\tau^2$ shown in equation (7.11). The degree to which the delta-function element dominates the pair determines the extent to which we can regard the turbulence response to boundary motion as an unimportant element of the flow, so now consider the extent to which this is likely to be the case.

The element of $\partial^2 G_1/\partial\tau^2$ which characterizes virtual mass effects,

$$-\frac{\partial^2}{\partial\tau^2}\left[\frac{\delta(t-\tau)}{2\pi|\mathbf{x}-\mathbf{y}|}\right],$$

is most easily dealt with because it is not subject to any 'pairing'. On convolution with $\zeta(\mathbf{y},\tau)$ in equation (7.10) its contribution to the pressure is simply

$$\frac{\rho}{2\pi}\int_\infty \frac{\partial^2\zeta}{\partial t^2}(\mathbf{y},t)\frac{d^2\mathbf{y}}{|\mathbf{x}-\mathbf{y}|}.$$

This indicates that the field induced by boundary acceleration is independent of both steady flow and boundary-layer effects.

The pairing applies only to the terms operated on by $\partial^2/\partial y_1\partial\tau$ and $\partial^2/\partial y_1^2$ and, since the relative magnitudes of the elements of each pair are strongly dependent on the length scales and frequencies of the surface motion, we will assume now that small amplitude boundary vibration occurs at frequency ω_0 and that the boundary movement is described by

$$\zeta(\mathbf{y},\tau) = \zeta(\mathbf{y})\,e^{-i\omega_0\tau}.$$

Consider first the elements of $\partial^2 G_1/\partial\tau^2$ operated on by $\partial^2/\partial y_1\partial\tau$, which we write as

$$-\frac{\partial^2}{\partial y_1\partial\tau}\left[\frac{U_1\delta(t-\tau)}{2\pi^2}\int_\infty \frac{e^{i\mathbf{k}.(\mathbf{x}-\mathbf{y})-2|\mathbf{k}|d}}{|\mathbf{k}|}d^2\mathbf{k}\right.$$
$$-\frac{U_1^2}{8\pi^2}\int_\infty \frac{|k_1|}{|\mathbf{k}|}\frac{(1+2e^{-2|\mathbf{k}|d})(1-e^{-2|\mathbf{k}|d})}{(1-e^{-4|\mathbf{k}|d})^{\frac{1}{2}}}\exp\left[-U_1\beta(ik_1(t-\tau)+\alpha|k_1|\,|t-\tau|)\right]$$
$$\left.\times\exp\left[-2|\mathbf{k}|d+i\mathbf{k}.(\mathbf{x}-\mathbf{y})\right]d^2\mathbf{k}\right] = -\frac{\partial^2}{\partial y_1\partial\tau}[P = P_1+P_2],$$

say, where P_1 is the delta function element of P

$$P_1 = \frac{U_1\delta(t-\tau)}{2\pi^2}\int_\infty \frac{e^{i\mathbf{k}.(\mathbf{x}-\mathbf{y})-2|\mathbf{k}|d}}{|\mathbf{k}|}d^2\mathbf{k},$$

and P_2 is the element with the more diffuse time dependence (and which we think is related to the level of turbulence response),

$$P_2 = -\frac{U_1^2}{8\pi^2}\int_\infty \frac{|k_1|}{|\mathbf{k}|}\frac{(1+2e^{-2|\mathbf{k}|d})(1-e^{-2|\mathbf{k}|d})}{(1-e^{-4|\mathbf{k}|d})^{\frac{1}{2}}}\exp\left[(-U_1\beta(iK_1(t-\tau)+\alpha|k_1|\,|t-\tau|)\right]$$
$$\times\exp\left[-2|\mathbf{k}|d+i\mathbf{k}.(\mathbf{x}-\mathbf{y})\right]d^2\mathbf{k}.$$

When these expressions are substituted into equation (7.10) and integrations performed by parts with respect to (y_1,τ), their contribution to the pressure may be written

$$\rho\int_\infty \zeta(\mathbf{y},\tau)\frac{\partial^2 P}{\partial y_1\partial\tau}d^2\mathbf{y}\,d\tau = \rho\int_\infty \frac{\partial^2\zeta}{\partial y_1\partial\tau}(\mathbf{y},\tau)P d^2\mathbf{y}\,d\tau = -i\rho\omega_0\int_\infty \frac{\partial\zeta}{\partial y_1}(\mathbf{y})\,e^{-i\omega_0\tau}P\,d^2\mathbf{y}\,d\tau.$$

We write this expression in the form of an integral with respect to wavenumber $\mathbf{k}$ as

$$\frac{\rho\omega_0}{(2\pi)^2}\int_\infty k_1\,\tilde{\xi}(-\mathbf{k})\,\tilde{P}(\mathbf{k},\tau)\,e^{-i\omega_0\tau}\,d^2\mathbf{k}\,d\tau \tag{7.14}$$

in order to emphasize the importance of length scale in our comparison. The contribution to (7.14) from the delta function element F_1 is

$$\frac{\rho\omega_0 U_1}{2\pi^2}\,e^{-i\omega_0 t}\int_\infty \frac{k_1}{|\mathbf{k}|}\,\tilde{\xi}(-\mathbf{k})\,e^{i\mathbf{k}.\mathbf{x}-2|\mathbf{k}|d}\,d^2\mathbf{k}, \tag{7.15}$$

and P_2's contribution is

$$-\frac{\rho\omega_0 U_1^3}{8\pi^2}\,e^{-i\omega_0 t}\int_\infty \tilde{\xi}(-\mathbf{k})\,\frac{k_1^3}{|\mathbf{k}|}\,\frac{(1+2e^{-2|\mathbf{k}|d})(1-e^{-2|\mathbf{k}|d})}{[(\omega_0-U_1\beta k_1)^2+(U_1\alpha\beta k_1)^2]}\,e^{-2|\mathbf{k}|d+i\mathbf{k}.\mathbf{x}}\,d^2\mathbf{k}. \tag{7.16}$$

The extent to which the pressure field is influenced by terms that describe the surface geometry at times other than the observation time, including times after the observation time, is determined by the magnitude of (7.16) relative to (7.15). If the two are of the same order, then we cannot guarantee that turbulence response will be an unimportant element of the boundary motion-induced pressure. On the other hand, if (7.16) is much smaller than (7.15), then the surface source terms to be evaluated at the observation time are the most important, and under those conditions there is no reason to suppose that turbulence response is an important element of the flow, because surface terms to be evaluated at times other than the observation time, and which might on causal grounds call for a turbulence response, are negligible.

The comparison, which should be at arbitrary $\mathbf{k}$, involves the ratio of the integrands in (7.16) and (7.15), i.e.

$$-\frac{U_1^2}{4}\,\frac{k_1^2(1+2e^{-2|k_1|d})(1-e^{-2|k_1|d})}{[(\omega_0-U_1\beta k_1)^2+(U_1\alpha\beta k_1)^2]}$$

or, in non-dimensional form,

$$-\frac{1}{4}\,\frac{\kappa_1^2(1+2e^{-2|\kappa|})(1-e^{-2|\kappa|})}{[(\Omega_0-\beta\kappa_1)^2+(\alpha\beta\kappa_1)^2]}.$$

The non-dimensionalizing variables are the flow's characteristic length and time scales, d and d/U_1. $\boldsymbol{\kappa} \equiv \mathbf{k}d$; $\Omega_0 \equiv \omega_0 d/U_1$.

At $\Omega_0 = 0$, this ratio has the value

$$-\tfrac{1}{2}(1+2e^{-2|\kappa|}),$$

so that turbulence response terms could then be very important. They are potentially even more so at $\Omega_0 = \beta\kappa_1$, when the phase speed of the surface wave elements and those of unstable waves on the 'vortex sheet' coincide. Then the ratio is

$$-\frac{(1+2e^{-2|\kappa|})}{(1+e^{-2|\kappa|})}.$$

At higher Strouhal numbers Ω_0 the ratio reduces progressively, and has the limiting form

$$-\frac{\kappa_1^2}{4\Omega_0^2}(1+2e^{-2|\kappa|})(1-e^{-2|\kappa|}),$$

which confirms the intuitively plausible result that when the surface waves are at high Ω_0, or more correctly at high phase speed $|\Omega_0/k_1^2|$, there is little scope for turbulence response.

In a similar way, the term-pair operated on by $\partial^2/\partial y_1^2$ consists of a delta-function element,

$$\frac{\rho U_1^2}{4\pi^2} e^{-i\omega_0 t} \int_\infty \frac{k_1^2}{|\mathbf{k}|} \tilde{\xi}(-\mathbf{k}) (1 - 2e^{-2|\mathbf{k}|d}) e^{-2|\mathbf{k}|d + i\mathbf{k}.\mathbf{x}} d^2\mathbf{k}, \tag{7.17}$$

and an element

$$\frac{\rho U_1^2}{8\pi^2} e^{-i\omega_0 t} \int_\infty \tilde{\xi}(-\mathbf{k}) \frac{k_1^3}{|\mathbf{k}|} (1 - e^{-2|\mathbf{k}|d}) (1 - 2e^{-2|\mathbf{k}|d}) \times \frac{(\omega_0 - U_1 k_1) e^{-2|\mathbf{k}|d + i\mathbf{k}.\mathbf{x}}}{[(\omega_0 - U_1 \beta k_1)^2 + (U_1 \alpha \beta k_1)^2]} d^2\mathbf{k} \tag{7.18}$$

from the diffuse time-integral. The ratio of the integrands, (7.18) divided by (7.17), of these expressions in non-dimensional form is now

$$\frac{1}{2} \frac{\kappa_1 (\Omega_0 - \kappa_1) (1 - e^{-2|\kappa|})}{[(\Omega_0 - \beta\kappa_1)^2 + (\alpha\beta\kappa_1)^2]}.$$

When $\Omega_0 = 0$, this ratio has the value -1, which indicates that when the boundary is rigid the two types of surface term cancel one another exactly. This confirms the anticipated result that the surface terms must vanish on a rigid, non-planar surface, the pressure field being given by the turbulence field alone. As Ω_0 is increased to the value $\Omega_0 = \beta\kappa_1$, the ratio is again -1, which suggests as before a strong turbulence response. The ratio is actually zero when $\Omega_0 = \kappa_1$, which indicates that these turbulence-response-related surface terms have no role to play when the boundary supports waves whose phase speed equals the velocity of the steady flow remote from the boundary. At high enough Strouhal number, the ratio again tends to zero, this time like

$$\frac{\kappa_1}{2\Omega_0} (1 - e^{-2|\kappa|}).$$

The behaviour when Ω_0 and κ_1 have opposite signs is of course less interesting, because those elements correspond to waves that propagate upstream, and they are inevitably less well coupled to the flow's instabilities. But the asymptotic behaviour of the various term pairs discussed above at both zero and infinite Strouhal number is the same.

It is only when the surface motion is at high Strouhal number, or, strictly, when the phase speed of the surface wave elements is high in comparison with the free-stream velocity of the flow, that we can confidently interpret the surface terms in a way that is uncomplicated by turbulence response. In this limit, the boundary pressure may be written down very simply, as in equation (7.9):

$$p(\mathbf{x}, t) = \int_\infty [T] d^3\mathbf{y}\, d\tau + \frac{\rho}{2\pi} \int_\infty \frac{\partial^2 \zeta}{\partial t^2}(\mathbf{y}, t) \frac{d^2\mathbf{y}}{|\mathbf{x} - \mathbf{y}|} + \frac{\rho}{2\pi} \int_\infty 2U_1 \frac{\partial^2 \zeta}{\partial y_1 \partial t}(\mathbf{y}, t) \frac{d^2\mathbf{y}}{(4d^2 + |\mathbf{x} - \mathbf{y}|^2)^{\frac{1}{2}}} - \frac{\rho U_1^2}{2\pi} \int_\infty \frac{\partial^2 \zeta}{\partial y_1^2}(\mathbf{y}, t) \left[\frac{1}{(4d^2 + |\mathbf{x} - \mathbf{y}|^2)^{\frac{1}{2}}} - \frac{2}{(16d^2 + |\mathbf{x} - \mathbf{y}|^2)^{\frac{1}{2}}} \right] d^2\mathbf{y}.$$

In this form the surface terms are exactly analogous to those encountered in previous extensions of the Lighthill theory, but they now incorporate the effects of a rudimentary boundary layer.

8. The dynamics of a baffled piston vibrating beneath a boundary layer

As an illustration of the implications of this result, we use it to estimate the impedance of a baffled, spring-mounted piston vibrating beneath a turbulent boundary-layer flow. The linearized potential problem has already been considered by Ffowcs Williams & Lovely (1975), who concluded that the main effect of flow was associated with the suction on the piston as it protrudes from the boundary. If the suction were below that necessary to cancel the spring stiffness, the effect of flow would be to reduce the resonance frequency. But, if it exceeded that value, flow would induce the instability and flutter of the piston. Unfortunately, Ffowcs Williams & Lovely were unable to offer a very accurate estimate of the suction reliazable in practice because they argued that it would be determined by boundary-layer effects. The analysis of that problem then, is well suited to our new flow modelling.

We start from the full expression for the surface pressure, which we integrate over the piston face to deduce the piston force. First we determine the minimum Strouhal number for negligible turbulence response. We find that this is approximately 2, and in what follows we assume that the oscillation takes place at at least this value of the Strouhal number.

Although the finite boundary-layer scale does indeed limit the piston force, we find that this is not the sole, or even the most important, boundary-layer effect. There are other features which simply cannot be anticipated from a potential modelling which neglects the boundary layer's existence and it is only in the limit of very large piston radius that there is no significant difference between the predictions of the two theories. We find that, for pistons whose ratio of radius a to boundary-layer scale d is less than about 5, the mean flow 'suction' on a piston standing proud of its baffle is actually a compression, so that the difference between the situations with and without the boundary layer is not just one of degree. In the potential flow with slip, the surface pressure, and therefore the piston force, is dominated by what is actually a steady flow effect: the abrupt changes in boundary geometry induce large local variations in surface velocity and correspondingly large surface pressures. But with a boundary layer, these steady flow effects are absent, and instead the surface pressure is simply that required to drive an oscillation of the mean flow momentum back and forth in unison with the boundary movements, momentum which is only established at some distance away from the boundary. The difference is significant enough to change the expected sign of the flow-induced force, with the result that a piston which has a ratio of piston radius to boundary-layer scale below a critical value does not flutter. On the contrary, flow *increases* its resonance frequency.

We would not expect our estimate of the force, or of the geometrical ratios at which the changes occur, to offer more than a general guide to the real situation. Nevertheless, reports do indicate that the resonance frequency of a single, baffled Helmholtz resonator does rise in the presence of a mean flow past the orifice, and by an amount consistent with what we would anticipate from our vortex sheet modelling of the flow.

8.1. *The piston force*

The surface consists of a circular piston set in an infinite, plane, rigid baffle

$$\zeta(\mathbf{x},t) = \eta(|\mathbf{x}|)\,H(a-|\mathbf{x}|)\,\phi(t).$$

We allow for an arbitrary piston shape η so that later we can determine how sensitive the results are to the piston geometry. The surface pressure, $p(\mathbf{x},t)$, is given by equation (6.1), with $\partial^2 G_1/\partial\tau^2$ as in equation (7.11). The piston force, $F(t)$, is the integral of $p(\mathbf{x},t)$ over the piston face:

$$\begin{aligned} F(t) &= \int_\infty p(\mathbf{x},t)\,H(a-|\mathbf{x}|)\,d^2\mathbf{x} \\ &= \int_\infty TH(a-|\mathbf{x}|)\,d^3\mathbf{y}\,d\tau\,d^2\mathbf{x} + I + F_F + F_H. \end{aligned}$$

T is written for the 'turbulent' volume terms. As before, I is the (virtual mass) $\times$ acceleration of the piston,

$$I = \frac{\rho}{2\pi}\frac{\partial^2\phi}{\partial t^2}\int_\infty \frac{\eta(|\mathbf{y}|)\,H(a-|\mathbf{x}|)\,H(a-|\mathbf{y}|)}{|\mathbf{x}-\mathbf{y}|}\,d^2\mathbf{x}\,d^2\mathbf{y}.$$

It is unaffected by flow. F_F is the flow-induced piston force proportional to the piston displacement at the observation time,

$$F_F = -\frac{\rho U_1^2}{2\pi}\int_\infty \left[\frac{1}{(4d^2+|\mathbf{x}-\mathbf{y}|^2)^{\frac{1}{2}}} - \frac{2}{(16d^2+|\mathbf{x}-\mathbf{y}|^2)^{\frac{1}{2}}}\right] \times H(a-|\mathbf{x}|)\,\frac{\partial^2\zeta}{\partial y_1^2}(\mathbf{y},t)\,d^2\mathbf{x}\,d^2\mathbf{y}. \quad (8.1)$$

F_H is the component which depends primarily on the piston displacement at times other than the observation time,

$$F_H = F_H\left(\frac{\partial^2\zeta}{\partial y_1\partial\tau}(\mathbf{y},\tau), \frac{\partial^2\zeta}{\partial y_1^2}(\mathbf{y},\tau)\right),$$

say. Since we believe that the ratio of F_H to F_F is a measure of the importance of turbulence response induced by piston movement, our first task is to quantify the relative magnitudes of F_F and F_H as a function of Strouhal number. We now do that for the particular case of the sharp-edged, flat-topped piston.

8.2. *The minimum Strouhal number for negligible turbulence response*

We rearrange equation (8.1) in the form

$$F_F = \frac{\rho U_1^2}{2\pi}\int_\infty \left[\frac{1}{(4d^2+|\mathbf{x}-\mathbf{y}|^2)^{\frac{1}{2}}} - \frac{2}{(16d^2+|\mathbf{x}-\mathbf{y}|^2)^{\frac{1}{2}}}\right]\delta(a-|\mathbf{x}|)\,\frac{x_1}{|\mathbf{x}|}\,\frac{\partial\zeta}{\partial y_1}(\mathbf{y},t)\,d^2\mathbf{x}\,d^2\mathbf{y}, \quad (8.2)$$

define $\cos\gamma = y_1/|\mathbf{y}|$, $\cos(\theta+\gamma) = x_1/|\mathbf{x}|$ and write equation (8.2) as

$$\begin{aligned} F_F &= \frac{\rho U_1^2}{2\pi}\int_0^\infty\int_0^{2\pi}\int_0^{2\pi}\left[\frac{1}{[4d^2+r^2+a^2-2ar\cos\theta]^{\frac{1}{2}}} - \frac{2}{[16d^2+r^2+a^2-2ar\cos\theta]^{\frac{1}{2}}}\right] \\ &\qquad \times ar\cos\theta\cos^2\gamma\,(\partial\zeta/\partial r)\,dr\,d\theta\,d\gamma, \\ &= -\frac{\rho U_1^2}{2}\int_0^\infty\int_0^{2\pi}\left[\frac{1}{[4d^2+r^2+a^2-2ar\cos\theta]^{\frac{1}{2}}} - \frac{2}{[16d^2+r^2+a^2-2ar\cos\theta]^{\frac{1}{2}}}\right] \\ &\qquad \times ar\cos\theta\,\frac{\partial\zeta}{\partial r}\,dr\,d\theta, \end{aligned}$$

where $r \equiv |\mathbf{y}|$ is the radial co-ordinate measured from the centre of the piston. We define the typical integral with respect to θ as

$$A(r,\epsilon^2) = \int_0^{2\pi} \frac{\cos\theta\, d\theta}{[\epsilon^2 + r^2 + a^2 - 2ar\cos\theta]^{\frac{1}{2}}}$$
$$= \frac{[(r+a)^2+\epsilon^2]^{\frac{1}{2}}}{ar}\left[\left(2 - \frac{4ra}{(r+a)^2+\epsilon^2}\right)\mathbf{K}\left(\left(\frac{4ra}{(r+a)^2+\epsilon^2}\right)^{\frac{1}{2}}\right) - 2\mathbf{E}\left(\left(\frac{4ra}{(r+a)^2+\epsilon^2}\right)^{\frac{1}{2}}\right)\right],$$

(see Gradshteyn & Ryzhik 1965, pp. 389, 948, 937 and 905). **K** and **E** are complete elliptic integrals of the first and second kind respectively, as defined by Gradshteyn & Ryzhik, p. 904.

Consequently, F_F is given by

$$F_F = -\frac{\rho U_1^2 a}{2}\int_0^\infty [A(r,\epsilon^2 = 4d^2) - 2A(r,\epsilon^2 = 16d^2)]\, r\frac{\partial\zeta}{\partial r}\, dr$$
$$= -\frac{\rho U_1^2}{2}\int_0^\infty \left[\{(r+a)^2+4d^2\}^{\frac{1}{2}}\left\{\left(2 - \frac{4ra}{(r+a)^2+4d^2}\right)\mathbf{K}\left(\left(\frac{4ra}{(r+a)^2+4d^2}\right)^{\frac{1}{2}}\right)\right.\right.$$
$$\left. - 2\mathbf{E}\left(\left(\frac{4ra}{(r+a)^2+4d^2}\right)^{\frac{1}{2}}\right)\right\}$$
$$- 2\{(r+a)^2+16d^2\}^{\frac{1}{2}}\left\{\left(2 - \frac{4ra}{(r+a)^2+16d^2}\right)\mathbf{K}\left(\left(\frac{4ra}{(r+a)^2+16d^2}\right)^{\frac{1}{2}}\right)\right.$$
$$\left.\left. - 2\mathbf{E}\left(\left(\frac{4ra}{(r+a)^2+16d^2}\right)^{\frac{1}{2}}\right)\right\}\right]\frac{\partial\zeta}{\partial r}\, dr.$$

Now,

$$\zeta(r,t) = H(a-r)\,\phi_0\, e^{-i\omega_0 t},$$

$$\frac{\partial\zeta}{\partial r}(r,t) = -\delta(a-r)\,\phi_0\, e^{-i\omega_0 t}$$

and so F_F is

$$F_F = \rho U_1^2 a X(Q)\,\phi_0\, e^{-i\omega_0 t},$$

say, where

$$X(Q) = \left[\frac{(1+2/Q^2)\,\mathbf{K}((1+1/Q^2)^{-\frac{1}{2}}) - 2(1+1/Q^2)\,\mathbf{E}((1+1/Q^2)^{-\frac{1}{2}})}{1+1/Q^2}\right.$$
$$\left. - 2\left\{\frac{(1+8/Q^2)\,\mathbf{K}((1+4/Q^2)^{-\frac{1}{2}}) - 2(1+4/Q^2)\,\mathbf{E}((1+4/Q^2)^{-\frac{1}{2}})}{1+4/Q^2}\right\}\right],$$

and Q is the ratio of piston radius to boundary-layer scale, a/d.

The corresponding expression for F_H is

$$F_H = -\rho U_1^2 a\phi_0 Q\, e^{-i\omega_0 t}\int_\infty \frac{\kappa_1^3 e^{-2|\boldsymbol{\kappa}|} J_1^2(Q|\boldsymbol{\kappa}|)\,(1-e^{-2|\boldsymbol{\kappa}|})\,(2\Omega_0 e^{-2|\boldsymbol{\kappa}|} + \frac{1}{2}\kappa_1(1-2e^{-2|\boldsymbol{\kappa}|}))}{|\boldsymbol{\kappa}|^3[(\Omega_0 - \beta\kappa_1)^2 + (\alpha\beta\kappa_1)^2]}$$
$$\times d^2\boldsymbol{\kappa}. \quad (8.3)$$

As before, the integral has been written in terms of the relevant dimensionless variables.

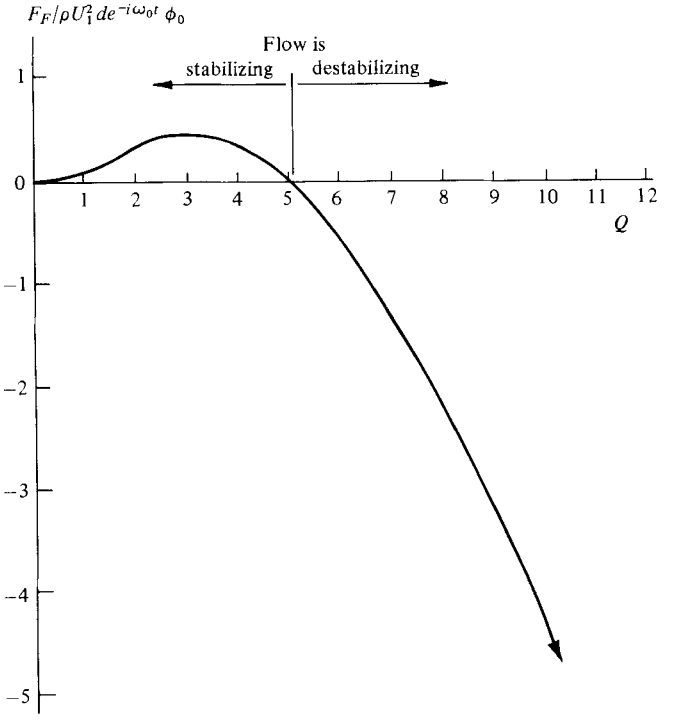

FIGURE 5. The flow-induced force F_F on a sharp-edged, baffled piston whose displaced amplitude is $\phi_0 e^{-i\omega_0 t}$. The oscillation is at high Strouhal number. This figure shows how F_F varies with the piston radius, a, at fixed boundary-layer scale, d. $F_F/\rho U_1^2 d e^{-i\omega_0 t}\,\phi_0$ is plotted against $Q(= a/d)$.

Equation (8.3) collapses to its known asymptotic limits at zero and infinite Strouhal number. If $\Omega_0 = 0$, F_H cancels F_F:

$$\begin{aligned}\lim_{\Omega_0 \to 0}[F_H] &= -\rho U_1^2 a \phi_0 Q\, e^{-i\omega_0 t} \int_\infty \frac{\kappa_1^2}{|\boldsymbol{\kappa}|^3} J_1^2(Q|\boldsymbol{\kappa}|)\,(1 - 2e^{-2|\kappa|})\, e^{-2|\kappa|}\, d^2\boldsymbol{\kappa} \\ &= -\rho U_1^2 a X(Q)\, \phi_0\, e^{-i\omega_0 t} \equiv -\rho U_1^2 d\, Q X(Q)\, \phi_0\, e^{-i\omega_0 t} \\ &= -F_F\end{aligned}$$

(see Gradshteyn & Ryzhik, p. 709). Also

$$F_H \to 0 \quad \text{as} \quad \Omega_0 \to \infty.$$

For finite values of Ω_0, the relative magnitudes of F_F and F_H can be deduced from figures 5 and 6. Those figures confirm our earlier conclusion that, the higher the Strouhal number, the less important turbulence response can be. At Strouhal numbers greater than approximately 2, it is evident that the response is negligible. In what follows, we shall restrict the Strouhal number to this and higher values, and so neglect F_H completely. The piston force then depends only on turbulent volume terms apparently uninfluenced by the piston movement, and on terms proportional to the piston displacement and acceleration at the observation time.

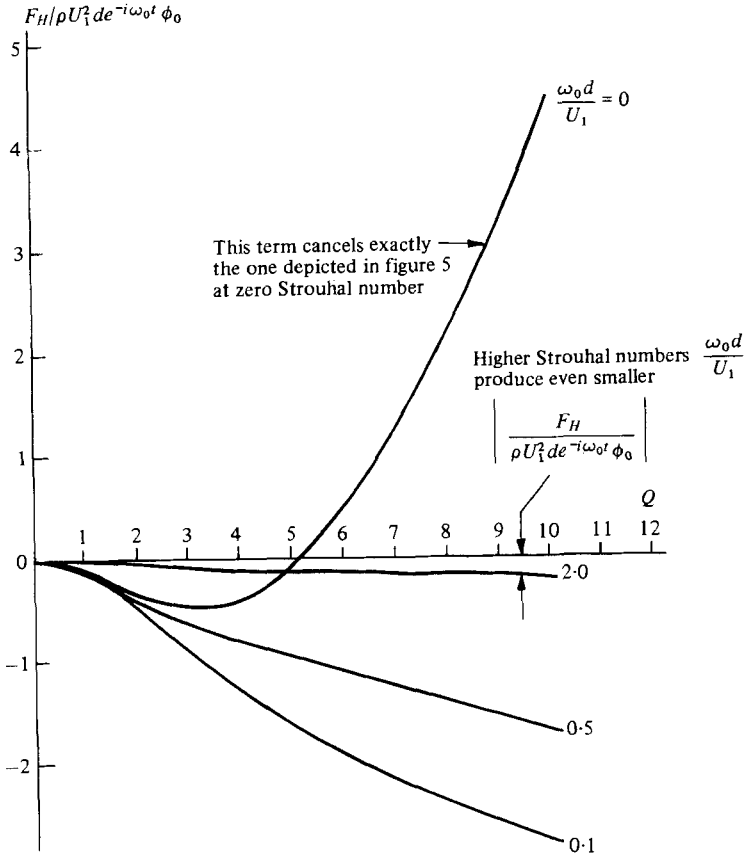

FIGURE 6. The turbulence-response-related surface terms become progressively less significant as the piston vibration Strouhal number rises.

8.3. *The effect of flow on the piston's apparent mechanical properties*

Fluid on one side of the baffle apparently increases the mass of a sharp-edged piston whose geometry is

$$\zeta(\mathbf{y}, t) = H(a - |\mathbf{y}|)\,\phi(t)$$

by an amount

$$\frac{I}{\partial^2\phi/\partial t^2} = \frac{\rho}{2\pi}\int_\infty \frac{H(a-|\mathbf{x}|)\,H(a-|\mathbf{y}|)}{|\mathbf{x}-\mathbf{y}|}\,d^2\mathbf{x}\,d^2\mathbf{y} = \tfrac{8}{3}\rho a^3$$

(Ffowcs Williams & Lovely 1975), while the flow induces a force of magnitude

$$F_F = \rho U_1^2 a X(Q)\,\phi(t)$$

proportional to the piston displacement. The total fluid-induced force is therefore

$$F(t) = \tfrac{8}{3}\rho a^3 \frac{\partial^2\phi}{\partial t^2} + \rho U_1^2 a X(Q)\,\phi.$$

In flow, the mass and spring stiffness, m and K, of the piston apparently assume new values m_u and K_u given by

$$m_u = m + \tfrac{8}{3}\rho a^3,$$

$$K_u = K + \rho U_1^2 a X(Q),$$

though of course m_u is independent of the flow velocity. So, if a piston resonates in quiescent fluid at a frequency

$$\omega = \left(\frac{K}{m+\frac{8}{3}\rho a^3}\right)^{\frac{1}{2}},$$

it does so in the presence of flow at a frequency

$$\omega_u = \left(\frac{K+\rho U_1^2 a X(Q)}{m+\frac{8}{3}\rho a^3}\right)^{\frac{1}{2}}.$$

In their potential modelling, Ffowcs Williams & Lovely noted that the flow-induced force would, in practice, be limited by boundary-layer effects to a value

$$\rho U_1^2 a\phi \ln(\epsilon/a),$$

where they identify ϵ as the 'length scale on which our potential modelling has broken down'. Our model is consistent with this in the large piston limit,

$$F_F \to \rho U_1^2 a\phi \ln(d/a) \quad \text{as} \quad Q = a/d \to \infty.$$

However, figure 5 reveals that this behaviour is characteristic only of pistons which have a very large radius or, equivalently, when the boundary layer is very thin. Pistons which have more moderate radii support flow-induced forces of the *opposite* sign. For pistons whose geometry is such that Q is less than about 5, the mean flow 'suction' on a piston standing proud of its baffle is actually a compression. In such cases, there can be no instability: on the contrary, flow *increases* a piston's resonance frequency.

At first sight, this appears to be a completely unphysical result, but it is less perplexing when one recalls that, although the flow-induced force is proportional to the piston displacement, it is not a steady force: the piston is oscillating at high Strouhal number – high enough to ensure that the profile of the adjacent boundary-layer flow vibrates back and forth in unison with the piston and without breaking up in doing so. Evidently, this mean flow-induced compression is simply the force required to push the mean flow away from the baffle. Equally, a suction would be induced on the piston were it recessed into its aperture, because it could drop below the level of the baffle only by pulling the mean flow towards it. It is only when the boundary layer is very thin that these features are eclipsed by the blockage effects that completely dominate the results from potential theory.

8.4. *Comparison with experiment*

The underlying mechanics which govern the vibration of a spring-mounted, baffled piston and that of a single, baffled, Helmholtz resonator (sketched in figure 7) are essentially the same. This is useful because it enables us to compare our predictions of the flow-dependent behaviour of a spring-mounted piston with published experimental measurements on Helmholtz resonators. In the Helmholtz resonator, the cavity offers a spring-like resistance to displacements at the neck; the virtual mass of fluid associated with the oscillatory flow in the neck is the counterpart of the piston's combined real and virtual masses. Thus, just like the baffled piston, the resonator can be assigned an effective spring stiffness K and a mass m, and its resonance frequency is

$$\omega_n = (K/m)^{\frac{1}{2}}.$$

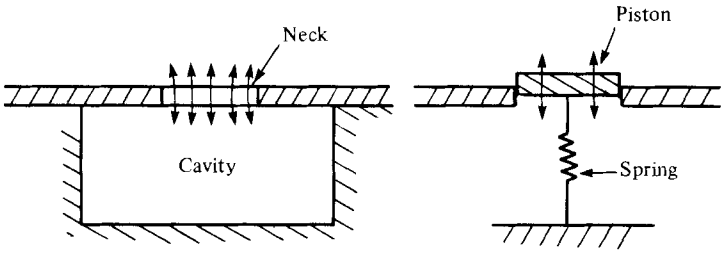

FIGURE 7. A Helmholtz resonator – equivalent to a piston on a spring.

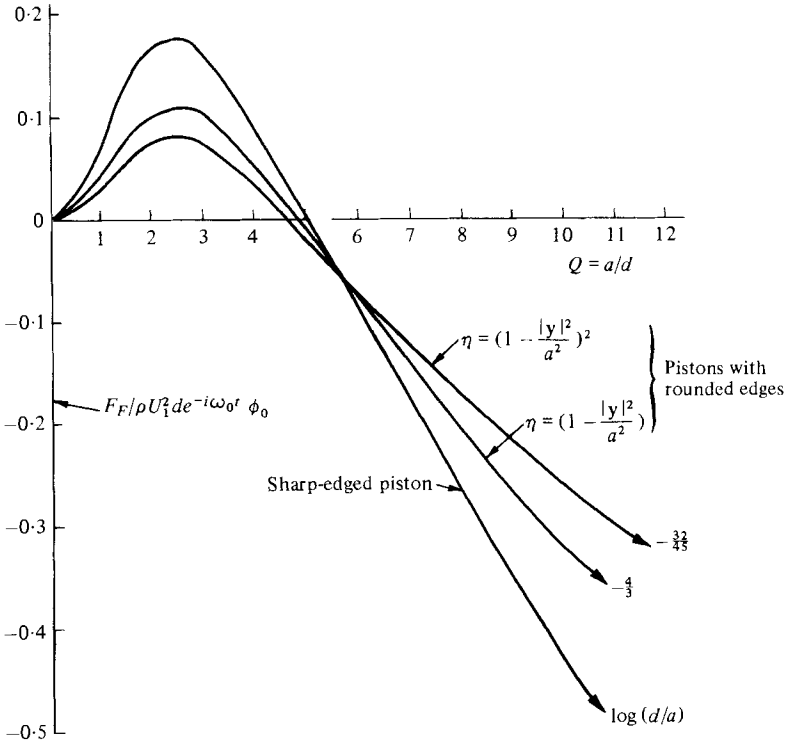

FIGURE 8. The flow-induced piston force as a function of piston geometry. Here the flat-topped, sharp-edged piston result is compared with results for two pistons with rounded edges. All are assumed to oscillate at high Strouhal number. This shows how the force on each piston changes as the boundary-layer scale is altered. As $d \to 0$ ($Q \to \infty$), which corresponds to no boundary layer, the forces have the limiting forms shown which is in agreement with Ffowcs Williams & Lovely (1975).

In the presence of flow, we would expect the analogy to hold, provided that the resonator orifice radius is not so large in comparison with the boundary-layer scale that there is a major flow interaction with the orifice. (Such an interaction would involve the vortex sheet shed at the orifice lip.) The fluid in the cavity and neck can then be thought of as a set of marked particles whose boundary with the external flow defines the shape of an equivalent 'piston', the motion of that defining the behaviour of the resonator under flow. However, since we have no idea of that piston's precise

shape, we must first establish how sensitive the mean-flow-induced force on a typical piston is to the specific piston geometry chosen.

Ffowcs Williams & Lovely showed how important edge geometry was in the potential problem by considering pistons of varying edge 'roundness'. We have calculated the corresponding forces in our vortex sheet analogy for the cases considered by them,

$$\zeta(\mathbf{y}, t) = \left(1 - \frac{|\mathbf{y}|^2}{a^2}\right) H(a - |\mathbf{y}|)\, \phi_0\, e^{-i\omega_0 t},$$

$$\zeta(\mathbf{y}, t) = \left(1 - \frac{|\mathbf{y}|^2}{a^2}\right)^2 H(a - |\mathbf{y}|)\, \phi_0\, e^{-i\omega_0 t},$$

and the results are given in figure 8. From this figure, it is evident that, although the level of the flow-induced force is different for each piston, as it is in the potential problem (due not only to the different edge geometries, but also because each piston displaces a different volume of fluid, the volumes being in the ratio $1 : \frac{1}{2} : \frac{1}{3}$), the force changes sign at approximately the same value of Q for all three pistons. The sign of the force is not at all sensitive to the precise piston geometry. We can therefore consider the effect of flow on the Helmholtz resonator with the confidence that, whatever the exact shape of the marked particle boundary, it has a negligible effect on the sign of the force and only a minor one on its magnitude.

There has been much experimental work on the flow-dependent acoustic properties of liners ever since their importance was drawn attention to by Meyer *et al.* (1958). Mechel's (1960) work shows that many possible effects exist in a given flow and that systematic study of any one of them is difficult. Different experimental techniques abound in the literature, ranging from the measurement of sound attenuation in ducts and subsequent inferences about the surface impedance (Mechel 1960), to measurements in individual orifices (e.g. Panton & Miller 1975). In choosing experimental results therefore we must select those which can be interpreted unambiguously. We must also confine our attention to tests on single, baffled resonators or, at any rate, arrays sparsely populated with holes, since the response of any given orifice is determined by the geometry of the array (Ffowcs Williams 1972).

Experiments in which the resonance frequency is measured as a function of the flow velocity are probably among the least susceptible to ambiguous interpretation. Furthermore, in such experiments, resonance frequencies do generally rise in the presence of flow, which is consistent with the idea of an additional flow-induced stiffness such as we have just found. It is therefore of interest to determine whether the parameter ranges in these experiments were such that we could have anticipated the results from our theory. There are two immediate questions. How is the length d to be defined, and is the Strouhal number high enough to ensure negligible turbulence response?

The buffer depth must be closely related to the thickness of the physical boundary layer that we are trying to model. At first sight, one might imagine that d should be set equal to the boundary-layer thickness, δ, defined, for example, as the distance from the boundary at which the mean velocity equals 99 % that of the free stream. But this is hardly reasonable, because of the characterically sharp initial rate of increase of mean velocity with distance from the boundary in turbulent boundary layers. Where the velocity profile satisfies a $\frac{1}{7}$-power law,

$$\frac{u}{U_1} = \left(\frac{x_3}{\delta}\right)^{\frac{1}{7}}$$

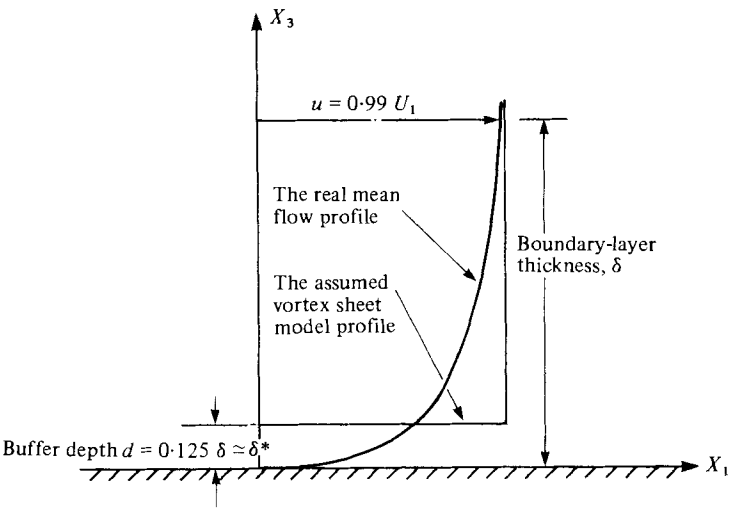

FIGURE 9. A diagram of how we expect to relate the geometry of our vortex sheet modelling to the mean flow profile (taken from Townsend 1976, p. 260) of a typical turbulent boundary layer. δ^* denotes the displacement thickness.

(Schlichting 1958), the local mean velocity u reaches half the free-stream value U_1 at a distance x_3 from the boundary less than 1 % of δ. Consequently, a modelling based on a buffer depth $d = \delta$ would much exaggerate the remoteness of the flow from the boundary.

Our interface must be positioned so that the boundary motion-induced volume source terms in expressions such as (4.6) are dominated by elements that are quadratic in the induced velocity field, rather than by linear source elements. Velocity perturbations that are driven by surface waves long on the boundary-layer scale are approximately uniform across the boundary layer, so that the linear source terms that arise in regions 1 and 2 of the flow can be made equal and opposite, so that they cancel, by setting the interface at one boundary-layer *displacement* thickness, δ^*, above the boundary. For shorter surface waves, whose induced velocity field falls away more sharply with distance from the boundary, an interface positioned closer to the boundary may well be preferable, but we do not expect our analysis to be able to handle that type of wave very accurately. Surface waves that are short on the scale of the boundary-layer thickness, δ, demand an explicit modelling of the boundary layer's profile. In our simpler vortex sheet model we must be content with a correct treatment of 'long' surface waves so that, rather than define d as the boundary-layer thickness δ, we propose to set it equal to the rather smaller displacement thickness δ^*. We think that this definition of the buffer depth is to be preferred to one that puts the interface in the free stream, clear of boundary-layer turbulence, even though it makes the requirement we specified earlier that the particle-attached interface should remain almost planar more difficult to justify.

In order to carry out an order-of-magnitude comparison between our theoretical results and reported experimental vehaviour, we need to specify a relationship between δ^* and δ likely to be representative of practical situations. For that, we take $\delta^* = \delta/8$, a ratio that actually applies to a boundary layer which satisfies a $\frac{1}{7}$th power law mean velocity distribution, though in fact is representative of many practical

Orifice radius a (mm)	Resonance frequency: No flow f_0 (Hz)	Resonance frequency: With flow f (Hz)	U_1 (m s^{-1})	Buffer depth d (mm)	$\frac{\omega d}{U_1}$	a/d	$\frac{K_{\text{flow}}}{0{\cdot}1\rho U_1^2 a}$	Author
4·76	250	350	80	1·4	0·04	3·30	0·77	Anderson (1977)
2·54	252	300	30	2·5	0·16	1·02	0·35	Panton & Miller
3·81	238	298			0·16	1·52	0·99	(1975)
5·08	211	249			0·13	2·03	1·12	
2·54	498	560			0·30	1·02	0·89	
3·81	472	520			0·27	1·52	1·25	
5·08	538	572			0·30	2·03	1·82	
5·0	760	860	60	2·1	0·19	2·42	0·52	Meyer, Mechel & Kurtze (1958)
4·0	1000	1450	80	2·1	0·23	1·94	0·54	Mechel (1960)

TABLE 1. Flow across the orifice of a baffled, Helmholtz resonator commonly causes its resonance frequency to rise. Our analysis shows that this comes about because the flow effectively increases the resonator stiffness, the existence of a boundary layer being crucial to the effect. Column 8 indicates the ratio of the flow-induced stiffness increase actually observed, K_{flow}, divided by our order-of-magnitude estimate for it, $0{\cdot}1\rho U_1^2 a$. $\omega = 2\pi f$.

boundary layers. Boundary-layer mean velocity profiles, which determine the relationship between δ^* and δ, are not unique of course, and are quite strongly influenced by such parameters as surface roughness, Reynolds number and the pressure gradient history of the boundary layer. Such effects will not, however, alter the value of this ratio by anything like an order of magnitude, so that setting $8\delta^* = \delta$ should be perfectly adequate for order-of-magnitude purposes. A vortex sheet model profile with $d = \delta/8$ superposed on the typical turbulent boundary-layer mean velocity profile given by Townsend (1976, p. 260) is illustrated in figure 9.

Experiments carried out in enclosed vessels can be handled in a similarly straightforward way because of the common features shared by the mean profiles in turbulent boundary layers and those in fully developed turbulent pipe flow and in 'two-dimensional' duct flow. In those cases, we set d equal to 12·5 % of the pipe radius and distance from duct wall to centre plane respectively. An orifice set in the wall of such vessels will only behave like an orifice set in a plane baffle if the orifice radius is not too large compared with the distance across the vessel, of course, but in fact this condition is quite often satisfied.

Experimental reports indicate that the relevant ratio a/d is commonly within the range 0 to 5. Consequently, for our order-of-magnitude estimate of the effect, we can take a mean value for F_F valid in that range. That value we take as $0{\cdot}1\rho U_1^2 a\phi_0$: a cavity spring stiffness K is effectively increased by flow to a value

$$K + 0{\cdot}1\rho U_1^2 a.$$

This flow-induced stiffness is in fact quite consistent with that observed experimentally. In column 8 of table 1 the ratio

$$\frac{K_{\text{flow}}}{0{\cdot}1\rho U_1^2 a}$$

is tabulated. This is the apparent increase in cavity stiffness needed to explain the experimental results K_{flow}, divided by the order-of-magnitude estimate of it from our

theory, so that a value of 1 implies perfect agreement. As the table shows, the sign and order of magnitude of the effects are unmistakably correct, and this despite the fact that the experimental Strouhal numbers are somewhat lower than the minimum value we specified for no significant turbulence response.

9. Conclusions

Because Lighthill's theory of aerodynamic sound does not explicitly recognize the existence of a boundary layer, its ability to account for mean flow effects correctly in analytical studies of boundary-layer noise is severely restricted. The correct modelling of discontinuous boundaries is particularly difficult in the Lighthill framework, which invariably emphasizes the surface singularities connected with the discontinuities, even though they would not feature in a real situation where a boundary layer cushions the mean flow from any abrupt surface irregularities. In this paper we have described a modelling which recognizes the existence of a boundary layer explicitly in an exact analogy between the real flow and one which has a step velocity profile. The mean velocity is zero near to the supporting surface, and is equal to the mean velocity of the real flow beyond a fixed distance from it.

The boundary layer's existence is thus recognized in the Green's function for the problem. The constraints which we impose at the interface of velocity discontinuity in the model give our Green's function the essential structure of the vortex sheet problem. In general, our source terms have the same form as those found in the usual aeroacoustic theory in that there are volume terms, taken to characterize the turbulence-induced pressure, and surface terms, which are assumed to describe boundary effects. The main difference is that, because of non-causal elements which have to be evaluated in future time, the volume terms, and hence the turbulence field, cannot be assumed known independently of boundary movement. That is an assumption implied in applications of Lighthill's theory which our analogy shows cannot be generally true. On causal grounds the turbulence must be capable of response to linear surface forcing. We suggest therefore that turbulent boundary-layer flows may well respond to linear stimulus in much the same way that free jets are now known to do.

The turbulence response to surface forcing is likely to be most significant when the surface motion is at low Strouhal number, based on mean flow velocity and boundary-layer scale, and may be particularly vigorous when the flow is driven by surface wave elements which share the phase speed of unstable waves on the vortex sheet. But, in the limit of high surface vibration Strouhal number, the surface terms assume a more familiar form. They are then dependent only on the boundary geometry and its rate of change at the observation time, and in this limit, although the 'turbulent' volume terms still contain elements to be evaluated in future time, there is no reason to suppose that they are perturbed by the surface vibration, so that the assumption usually made in Lighthill's theory (that turbulence and surface movements can be specified independently) applies once more.

Because of the interdependence between surface and volume terms, applications of the theory to boundary-layer flow noise may need to be posed in a novel way, although there appears to be no basic difficulty of principle. Indeed it appears that the analogy might be used in essentially the same way that similar non-causal jet noise analogies are now being used to predict the sound fields radiated by turbulent jets.

We conclude the paper with an illustration of our high Strouhal number estimate of boundary-layer fluid loading applied to a problem in which previous extensions of Lighthill's theory have failed to predict results which are observed experimentally. We estimate the impedance of a baffled piston vibrating beneath a boundary-layer flow, which is an appropriate model of a baffled Helmholtz resonator of the type widely used in the construction of acoustic liners. Experimentally, the resonance frequencies of such resonators are found to rise in the presence of a grazing flow. Existing theory predicts that the opposite should be true. Our analogy confirms that the boundary layer is responsible for the discrepancy and that a correct prediction of resonator behaviour is obtained once the existence of the boundary layer is recognized. Blockage effects, the main features to emerge from the previous modelling, dominate the problem when surface features are very large on the boundary-layer scale. But the boundary layer is important if the surface features are of a smaller scale, so that in the baffled piston problem, provided that the piston radius is not too large on the scale of the boundary layer, the flow effectively augments the resonator stiffness. The piston can move only by pushing the mean flow away from, or drawing it towards, the baffle, and it does so through the cushioning effect of the boundary layer. That layer imposes its own complicated character on the problem, a character that we are only beginning to understand.

This work was carried out while M.P. was a Research Student supported by the Science Research Council. That support is gratefully acknowledged.

REFERENCES

ANDERSON, J. S. 1977 The effect of an air flow on a single side branch Helmholtz resonator in a circular duct. *J. Sound Vib.* **52**, 423.

BENJAMIN, T. B. 1964 Fluid flow with flexible boundaries. *Proc. 11th Int. Cong. Appl. Mech., Munich*, p. 109.

CRIGHTON, D. G. 1968 Wave motion and vibration induced by turbulent flow. Ph.D. thesis, University of London.

CURLE, N. 1955 The influence of solid boundaries upon aerodynamic sound. *Proc. Roy. Soc.* A **231**, 412.

DOWLING, A. P., FFOWCS WILLIAMS, J. E. & GOLDSTEIN, M. E. 1978 Sound production in a moving stream. *Phil. Trans. Roy. Soc.* A **288**, 321.

FFOWCS WILLIAMS, J. E. 1965 Sound radiation from turbulent boundary layers formed on compliant surfaces. *J. Fluid Mech.* **22**, 347.

FFOWCS WILLIAMS, J. E. 1966 The influence of simple supports on the radiation from turbulent flow near a plane compliant surface. *J. Fluid Mech.* **26**, 641.

FFOWCS WILLIAMS, J. E. 1972 The acoustics of turbulence near sound absorbent liners. *J. Fluid Mech.* **51**, 737.

FFOWCS WILLIAMS, J. E. 1974 Sound production at the edge of a steady flow. *J. Fluid Mech.* **66**, 791.

FFOWCS WILLIAMS, J. E. & LOVELY, D. J. 1975 Sound radiation into uniformly flowing fluid by compact surface vibration. *J. Fluid Mech.* **71**, 689.

GOLDSTEIN, M. E. 1976 *Aeroacoustics*. McGraw-Hill.

GRADSHTEYN, I. S. & RYZHIK, I. M. 1965 *Table of Integrals, Series and Products*, 4th edn. Academic.

JONES, D. S. 1973 The effect of radiation due to a moving source on a vortex sheet. *Proc. Roy. Soc. Edinb.* **72** (14), 195.

LANDAHL, M. T. 1967 A wave guide model for turbulent shear flow. *J. Fluid Mech.* **29**, 441.

LIGHTHILL, M. J. 1952 On sound generated aerodynamically. I. General theory. *Proc. Roy. Soc.* A **211**, 564.

LILLEY, G. M. 1974 On the noise from jets. *AGARD Conf. Proc.* no. 131, paper 13.

LOVELY, D. J. 1974 Novel methods of aerodynamic sound generation. Ph.D. thesis, University of London.

MANI, R. 1976 The influence of jet flow on jet noise. Part I. The noise of unheated jets. *J. Fluid Mech.* **73**, 753.

MECHEL, F. 1960 Schalldämpfung and Schallverstärkung in Luftströmungen durch absorbierend ausgekleidete Kanale. *Acustica* **10**, 133.

MEYER, E., MECHEL, F. & KURTZE, G. 1958 Experiments on the influence of flow on sound attenuation in absorbing ducts. *J. Acoust. Soc. Am.* **30**, 165.

MOORE, C. J. 1977 The role of shear layer instability waves in jet exhaust noise. *J. Fluid Mech.* **80**, 321.

MORFEY, C. L. & TESTER, B. J. 1976 Developments in jet noise modelling. *J. Sound Vib.* **46**, 79.

MORGAN, J. D. 1975 The interaction of sound with a subsonic cylindrical vortex layer. *Proc. Roy. Soc.* A **344**, 341.

PANTON, R. L. & MILLER, J. M. 1975 Excitation of a Helmholtz resonator by a turbulent boundary layer. *J. Acoust. Soc. Am.* **58**, 800.

POWELL, A. 1960 Aerodynamic noise and the plane boundary. *J. Acoust. Soc. Am.* **32**, 982.

SCHLICHTING, H. 1955 *Boundary Layer Theory*. Pergamon.

TOWNSEND, A. A. 1976 *The Structure of Turbulent Shear Flow*, 2nd edn. Cambridge University Press.